CEBAF-TH-92-08
NSF-ITP-90-234
DOE/ER/40423-23
LAUR-91-617

Lattice calculation of $I = 2$ pion scattering length

Stephen R. Sharpe[a,b,c], Rajan Gupta[a,d] and Gregory W. Kilcup[a,e]

a) *Institute for Theoretical Physics, University of California, Santa Barbara, CA 93106*

b) *Continuous Electron Beam Accelerator Facility, Newport News, VA 23606*

c) *Physics Department, University of Washington, Seattle, WA 98195*

d) *T-8, MS-B285, Los Alamos National Laboratory, Los Alamos, NM 87545*

e) *Physics Department, The Ohio State University, Columbus, OH 43210*

Abstract

We present results for the $I = 2$ pion scattering length calculated using staggered fermions in the quenched approximation. The calculation uses the finite volume dependence of the energy of a two pion state. We find good agreement with current algebra predictions for scattering of Goldstone pions, and reasonable agreement for the non-Goldstone pions.

March 1992

1. Introduction

Lattice studies of QCD have, for the most part, considered the properties of stable single-particle states. It is clear, however, that if lattice QCD is to become a quantitative calculational tool, a study of resonances and scattering amplitudes is crucial. For example, to calculate non-leptonic weak decay amplitudes such as $K \to \pi\pi$ one must understand the interactions between the pions in the final state, and the possible appearance of resonances.

There are a number of problems which make such calculations difficult. In general scattering and decay amplitudes are complex, and are thus only related indirectly to the real quantities evaluated in Euclidean functional integrals. An example of an explicit relationship has been given by Lüscher for two-body scattering amplitudes below the inelastic threshold [1] [2]. Lüscher shows how the finite volume dependence of the two particle energy levels in a sufficiently large cubic box is related to the phase shifts.[1] For decay amplitudes such as $\mathcal{A}(K \to \pi\pi)$ there is, in addition, the problem of projecting against $\pi\pi$ states of lower energy than that required for the physical amplitude, as has been clarified by Maiani and Testa [5]. Proposals for dealing with these problems have been discussed by Michael [6], Wiese [7], DeGrand [8] and Lüscher [9].

The restriction to stable single particle states is also due in part to the lack of adequate computer power. Full QCD has many resonances in its spectrum, for example the rho meson. Present simulations, however, involve heavy quark masses and use relatively small volumes, so that the rho is kinematically stabilized: $m_\rho < 2\sqrt{m_\pi^2 + p_{\rm min}^2}$, $p_{\rm min} = 2\pi/L$. Large scale calculations are possible in the quenched approximation, but here potential resonances may be artificially stabilized by the absence of quark loops.

In this paper we calculate the $I = 2$ $\pi\pi$ scattering amplitude at threshold, using the finite volume shift in the energy of the lightest two pion state, i.e. the method of Refs. [1] and [4]. This is among the simplest two body calculations possible as it avoids many of the complications just mentioned. In particular, since the amplitude at threshold is real, it can be, and in fact is, directly related to the finite volume energy shift. Furthermore, since we are studying the two pion state of lowest energy, other states are automatically damped in Euclidean space. We choose the $I = 2$ channel since it involves quark and gluon exchanges, but no quark annihilation, so that no essential feature of the calculation is lost when using the quenched approximation. Finally, we study pions rather than heavier particles, e.g. rhos, since the signal for pions is much better.

Despite these simplifications one can still learn much from the calculation. As shown long ago by Weinberg [10], PCAC predicts the leading chiral behavior of the scattering amplitude, and we can test the lattice results against this prediction. To be more precise, we test the generalization of Weinberg's result appropriate to a theory with four degenerate quarks. We use the staggered formulation of lattice fermions, for which one can derive the expected chiral behavior directly on the lattice, provided that one uses external pseudo-Goldstone pions and makes some non-trivial assumptions [11]. Our calculation thus tests these assumptions. We can also study the breaking of the staggered flavor symmetry by comparing scattering of Goldstone and non-Goldstone pions. The latter are not constrained by lattice Ward identities. Finally, we can study the approach to the chiral limit by determining the size of the corrections from terms higher order in m_π^2.

Intrinsic to the calculation is the use of finite volume dependence. Finite volume studies are likely to be a major tool in future simulations, so it is important to see that one of the simplest calculations can be done.

It turns out that, although the essential idea is simple, the interpretation of the results is not straightforward. This is partly due to our use of staggered fermions, which quadruples the number of flavors. The main complications are caused, however, by the details of the wall sources we use for our propagators. Because of this, we break the discussion up into sections in such a way that it is clear which complications are specific to all fermion types, which to staggered fermions in general, and which to our particular calculation.

[1] There is a long history of such studies of quantum mechanics in a spherical volumes, e.g. Ref. [3]. In the context of lattice field theories, the leading term in an infinite volume expansion was first given in Ref. [4].

The article is organized as follows. We begin, in section 2, by establishing notation and outlining the method. In section 3 we discuss the relationship between the two flavor and four flavor scattering amplitudes. This is a necessary prelude to an explanation of the predictions of chiral symmetry for SU(2) and SU(4) scattering lengths, which we give in section 4.

Up to this point the discussion applies to both staggered and Wilson fermions. Section 5 discusses the complications which arise from using staggered fermions. Section 6 explains how we actually do the calculation, and how we deal with the additional complications that our method introduces. In section 7 we present our results, and, we end, in section 8, with our conclusions.

We devote three appendices to subjects somewhat off the main line of development. Appendix A gives a simplified summary of Lüscher's analysis [1], from which we extract some results needed to deal with the complications introduced by staggered fermions. In appendix B, we derive the chiral behavior of the scattering amplitudes on the lattice for staggered fermions. The derivation also allows us to see explicitly the relationship between the finite volume energy shift and the scattering amplitude. Finally, in appendix C we give a transfer matrix interpretation of the correlator that we calculate.

The first calculation of pion scattering lengths was attempted by Guagnelli, Marinari and Parisi [12]. They found a clear signal for the finite volume energy shift with both Wilson and staggered fermions, and verified the expected finite volume dependence. The major drawback with their calculation was that they did not evaluate all of the diagrams contributing to $I = 2$ pion scattering. As explained in section 6, this means that their results are not simply related to any physical quantity.

A preliminary discussion of this work was given in Ref. [13]. While the numerical results have not changed, our understanding of the theoretical issues has improved, and we correct in the following various errors made in Ref. [13].

2. Overview

An ideal calculation would extract scattering amplitudes from four-point functions in the textbook manner, *i.e.* by going to the pion poles and isolating the residue. In principle one could imagine doing the required analytic calculation from the Euclidean space Green functions of lattice QCD, but in practice finite statistical errors preclude this possibility. Instead we settle for a simpler calculation which obtains only the pion scattering amplitude at threshold.

The basic idea is to calculate the lowest energy of a two pion state in a cubic box of length L with periodic boundary conditions. As the volume is reduced from infinity, this energy differs from $2m_\pi$ by a factor which varies inversely with the volume. In Ref. [1] Lüscher derived the precise form of this factor

$$\delta E = E - 2m_\pi = -\frac{4\pi a_0}{m_\pi L^3}\left(1 + c_1\frac{a_0}{L} + c_2\left(\frac{a_0}{L}\right)^2\right) + O(1/L^6)\ . \qquad (2.1)$$

Here a_0 is S-wave scattering length, defined in terms of the phase shift by $a_0 = \lim_{p\to 0}\delta/p$. The numerical coefficients are $c_1 = -2.837297$ and $c_2 = 6.375183$. The result (2.1) is an expansion of a general formula valid in all volumes as long as $L > 2R$, where R is the range of the interaction [2]. The general formula shows that E is a function of the scattering length alone only up to the order shown. The terms of $O(1/L^6)$ depend in addition on the effective range (i.e. the $O(p^3)$ term in $\delta(p)$). At $O(1/L^9)$ one also requires the $O(p^5)$ term in $\delta(p)$, and the $l = 4$ phase shift enters at $O(1/L^{11})$. In this paper we use the form Eq. (2.1) keeping only terms up to $1/L^5$.

We prefer to express the energy shift in terms of the non-relativistically normalized scattering amplitude at threshold, $T = -4\pi a_0/m_\pi$,

$$\delta E = \frac{T}{L^3}\left(1 - c_1\frac{m_\pi T}{4\pi L} + c_2\left(\frac{m_\pi T}{4\pi L}\right)^2\right) + O(L^{-6})\ . \qquad (2.2)$$

T is related to the relativistically normalized amplitude T^R, by $T = -T^R/(4m_\pi^2)$. (In Ref. [13] the opposite sign for T was used. The present usage agrees with the standard definition, of, for example, Ref. [1].) In appendix A we discuss

why using T rather than a_0 simplifies the physical interpretation of δE. We also give a heuristic explanation of the origin of the terms of order T^2 and T^3.

In principle it is straightforward to calculate E. We use the Euclidean space correlator

$$C_{\pi\pi}(t) = \langle \sum_{\vec{x}_1} \mathcal{O}_1(\vec{x}_1, t) \sum_{\vec{x}_2} \mathcal{O}_2(\vec{x}_2, t) \mathcal{S}_3(\vec{x}_3, t=0) \mathcal{S}_4(\vec{x}_4, t=0) \rangle \ , \qquad (2.3)$$

where the sources $\mathcal{S}_i$ and the operators $\mathcal{O}_i$ respectively create and destroy pions of flavor "i". For example, to destroy a π^+ we use $\mathcal{O} = \bar{d}\gamma_0\gamma_5 u$. The expectation value indicates the usual functional integral over gauge and fermion fields, which we do in the quenched approximation, and with u and d quarks degenerate. A detailed description of operators and sources is given in section 6. For the present, we need only know that both the source (at time $t=0$) and the sink (at t) couple to the lowest energy two pion state. This means that at large $|t|$ the correlator will fall as

$$C_{\pi\pi}(t) = Z_{\pi\pi} \exp(-E|t|) + \dots \ , \qquad (2.4)$$

(the ellipsis indicating terms suppressed exponentially) from which we can extract E.

To obtain δE we need m_π, and this we calculate in the usual way using the two point function

$$C_\pi(t) = \langle \sum_{\vec{x}_4} \mathcal{O}_1(\vec{x}_1, t) \mathcal{S}_1(\vec{x}_4, t=0) \rangle = Z_\pi \exp(-m_\pi|t|) + \dots \ . \qquad (2.5)$$

It is most useful in practice to combine Eqs. (2.4) and (2.5)

$$R(t) = \frac{C_{\pi\pi}(t)}{C_\pi(t)^2} = \frac{Z_{\pi\pi}}{Z_\pi^2} \exp(-\delta E|t|) + \dots \ . \qquad (2.6)$$

It is from such ratios that we extract δE.

The method of calculation is straightforward in principle, not differing essentially from the calculation of hadron masses. One must only take care to project onto a two pion state of definite isospin, as discussed in the following

section. The only practical concern is the possibility of contamination in $R(t)$ from excited states. It turns out, in our calculations, that $|\delta E t_{\max}| << 1$ ($t_{\max}$ being the maximum time separation used to extract the result), so that we can expand the exponential in R

$$R(t) = \frac{Z_{\pi\pi}}{Z_\pi^2} \left(1 - \delta E|t| + O(|t|^2)\right) + \dots \ , \qquad (2.7)$$

To extract the linear term proportional to δE one must work in a regime where t is small enough that $t\delta E \ll 1$, and at the same time t is large enough that the contributions of excited states are exponentially suppressed. For the numerical data we discuss below, there is indeed such a range of t where the linear term suffices. Were it not for additional complications related to the use of staggered fermions, the simultaneous extraction of δE and $Z_{\pi\pi}/Z_\pi^2$ would then be straightforward.[2]

3. Flavor symmetries

The four possible types of contractions contributing to $C_{\pi\pi}$ are shown in Fig. 1. We refer to the contractions respectively as the "direct" or "gluon exchange" diagram (Fig. 1a), the "crossed" or "quark exchange" diagram (Fig. 1b), "single annihilation" (Fig. 1c), and "double annihilation" or "glueball" (Fig. 1d). Since the operators $\mathcal{O}_1$ and $\mathcal{O}_2$ in Eq. (2.3) are summed over all space, there is no distinction between "quark exchange" and "anti-quark exchange" diagrams. Similarly, charge conjugation does not change the amplitudes, so that the direction of the arrows is unimportant. Thus all contractions can be expressed in terms of the correlators represented by these four diagrams. We refer to the contributions of each diagram to the ratio $R(t)$ as $D(t)$, $C(t)$, $A(t)$ and $G(t)$ (for glueball) respectively.

We first consider the scattering of physical pions in QCD. Two pions in an S-wave can have isospin 0 or 2, and we label the corresponding amplitudes

[2] This point was misunderstood in Ref. [13], where it was suggested, incorrectly, that independent knowledge of $Z_{\pi\pi}/Z_\pi^2$ is necessary. We thank Claude Bernard for pointing this out.

at threshold T_0 and T_2, respectively. To obtain T_2 we study $\pi^+\pi^0$ scattering; the $I = 1$ part of this combination does not contribute since we use a spatially symmetric operator to create the pair. Only the direct and crossed contractions contribute, with the latter coming in with a relative minus sign because of Fermi statistics.[3] Thus we have

$$R_2(t) = D(t) - C(t) \,, \tag{3.1}$$

where the subscript on R denotes the isospin. On the other hand, extracting the $I = 0$ amplitude requires calculating all four diagrams

$$R_0(t) = D(t) + \tfrac{1}{2}C(t) - 3A(t) + \tfrac{3}{2}G(t) \,. \tag{3.2}$$

We consider only R_2 in this paper, since the direct and crossed diagrams require no more quark propagators than spectrum calculations, and can thus be done with present resources. To evaluate the annihilation diagrams, by contrast, would require many more propagator calculations.

Our calculation is done in the quenched approximation, i.e. we do not include internal quark loops. For the single and double annihilation diagrams, quark loops are needed to make the scattering amplitudes unitary. In Euclidean space the lack of unitarity implies that $R_0(t)$ will not behave as a pure exponential for long times, instead growing linearly with t. This is shown in an explicit example in appendix B. This problem does not, however, afflict the direct and crossed diagrams which are needed for R_2. Of course the results obtained in the quenched approximation will differ from those in the full theory, but for the direct and crossed diagrams no essential part of the physics is lost by using the quenched approximation.

Since we can calculate $D(t)$ and $C(t)$ separately, we can form $D + C$ as well as $R_2 = D - C$. It is thus interesting to determine the physical quantity corresponding to $D + C$. It turns out that to do this one has to consider a

[3] We find it convenient to keep this sign explicit and have the lines in Fig. 1 correspond to the quark propagators we actually calculate.

theory with four degenerate flavors. We give a brief discussion of the two-pion correlators in such a theory.

Four flavors is the minimum number allowing one to separate each of the diagrams in Fig. 1. For example, labeling the flavors u, d, s and c, the choices

$$\begin{aligned}
D: &\quad \mathcal{O}_1 = \overline{u}\gamma_5 d, \quad \mathcal{O}_2 = \overline{s}\gamma_5 c, \quad \mathcal{S}_3 = \overline{d}\gamma_5 u, \quad \mathcal{S}_4 = \overline{c}\gamma_5 s \,, \\
C: &\quad \mathcal{O}_1 = \overline{u}\gamma_5 d, \quad \mathcal{O}_2 = \overline{s}\gamma_5 c, \quad \mathcal{S}_3 = \overline{c}\gamma_5 u, \quad \mathcal{S}_4 = \overline{d}\gamma_5 s \,, \\
A: &\quad \mathcal{O}_1 = \overline{u}\gamma_5 d, \quad \mathcal{O}_2 = \overline{d}\gamma_5 c, \quad \mathcal{S}_3 = \overline{s}\gamma_5 u, \quad \mathcal{S}_4 = \overline{c}\gamma_5 s \,, \\
G: &\quad \mathcal{O}_1 = \overline{u}\gamma_5 d, \quad \mathcal{O}_2 = \overline{d}\gamma_5 u, \quad \mathcal{S}_3 = \overline{s}\gamma_5 c, \quad \mathcal{S}_4 = \overline{c}\gamma_5 s \,,
\end{aligned} \tag{3.3}$$

for the operators in Eq. (2.3) yield, respectively, Figs. 1a, b, c and d (with Figs. 1b and 1c being produced with a minus sign from Fermi statistics). The SU(4) representations that contribute to these correlators are those which appear in the product of two 15-dimensional adjoints. For S-wave scattering we need only the symmetric part:

$$(\mathbf{15} \times \mathbf{15})_{\text{symm}} = \mathbf{1} + \mathbf{15} + \mathbf{20} + \mathbf{84}. \tag{3.4}$$

The singlet is similar to the $I = 0$ channel for flavor SU(2), and is contained in all four types of contraction shown in Fig. 1. The **15** is contained in Figs 1a, b and c, but not in Fig. 1d, which is purely singlet. We are interested here in the **20** (⊞) and **84** (⊞□), for these are contained only in Figs. 1a and 1b. These two representations are distinguished by their symmetry under quark (or antiquark) interchange: the **84** is symmetric while the **20** is antisymmetric. Including the sign from Fermi statistics, this means that $R(\mathbf{84}) = D - C$ while $R(\mathbf{20}) = D + C$.

We conclude that $D - C$ gives us the scattering amplitude both for the $I = 2$ representation in SU(2) and the **84** representation in SU(4), while $D + C$ corresponds to the **20** representation of SU(4). In the quenched approximation, when the ensemble of gauge configurations is independent of the number of flavors, this implies that $T_2 = T(\mathbf{84})$. Of course, if one includes quark loops, the gauge configurations for the two theories will differ, and T_2 and $T(\mathbf{84})$ need not be the same. Nevertheless, as we discuss in the next section, chiral

symmetry implies a lowest order relationship between T_2 and $T(\mathbf{84})$ even when we include quark loops.

For staggered fermions we need to extend this discussion to the flavor group $SU(16)$. This is straightforward for all flavor groups $SU(N > 4)$. The decomposition of two adjoints is as in Eq. (3.4), i.e. a singlet, an adjoint, and the generalizations of the **84** and **20**. The latter two representations are distinguished by their symmetry under quark exchange, and we refer to them as **S** and **A**, respectively. In general their dimensions are $(N-1)N^2(N+3)/4$ and $(N-3)N^2(N+1)/4$ respectively. In the quenched approximation, the scattering amplitudes for all $N > 4$ are related to those discussed above by $T(\mathbf{S}) = T_2$ and $T(\mathbf{A}) = T(\mathbf{20})$.

4. Chiral predictions

Using $SU(2)_L \times SU(2)_R$ chiral symmetry, the amplitude T_2 can be expressed as

$$T_2 = \frac{1}{4f_\pi^2} + O(m_\pi^2 \ln(m_\pi^2)) \ , \tag{4.1}$$

in the normalization in which $f_\pi = 93$ MeV. The leading term, which is more familiar as $T_2^R = -m_\pi^2/f_\pi^2 + \ldots$, was given long ago by Weinberg [10]. The fact that T_2 is positive implies a repulsive interaction between the two pions. The non-leading terms (which include non-analytic chiral logarithms) have been classified by Gasser and Leutwyler, and can be partly, though not completely, written in terms of other physical quantities [14]. In a three flavor theory there are also non-leading terms proportional to $O(m_K^2 \ln(m_K))$.

As discussed in the previous section, we can also calculate the scattering amplitudes for both **S** and **A** representations for theories with $SU(N \geq 4)$ flavor symmetry, in the quenched approximation. Thus it is interesting to derive the expected chiral behavior of these amplitudes. This is a straightforward exercise in chiral perturbation theory. At leading order the chiral Lagrangian is, in Euclidean space,

$$\mathcal{L} = -\frac{f_\pi(N)^2}{4} \mathrm{Tr}\left(\partial_\mu \Sigma \partial_\mu \Sigma^\dagger\right) + \frac{f_\pi(N)^2}{2} \mu \, \mathrm{Tr}\left(M(\Sigma + \Sigma^\dagger)\right) \ , \tag{4.2}$$

where $\Sigma = \exp(2i\pi_a T_a / f_\pi(N))$ in terms of the N^2-1 pseudo-Goldstone bosons fields π_a. The group generators T_a are normalized to $\mathrm{Tr}(T_a T_b) = \frac{1}{2}\delta_{ab}$. M is the quark mass matrix, in terms of which the pion mass matrix is $(m_\pi^2)_{ab} = 4\mu \, \mathrm{Tr}(M T_a T_b)$. The only N dependence enters implicitly through $f_\pi(N)$, which is the physical parameter appropriate to a theory with an $SU(N)$ flavor symmetry. The scattering amplitudes are obtained from the π^4 term in $\mathcal{L}$, and we find

$$\begin{aligned} T(\mathbf{S}) &= \frac{1}{4f_\pi(N)^2} + O(m_\pi^2 \ln(m_\pi^2)) \ , \\ T(\mathbf{A}) &= -\frac{1}{4f_\pi(N)^2} + O(m_\pi^2 \ln(m_\pi^2)) \\ &= -T(\mathbf{S}) + O(m_\pi^2 \ln(m_\pi^2)) \ . \end{aligned} \tag{4.3}$$

Comparing this with Eq. (4.1) we see that the expressions for T_2 and $T(\mathbf{S})$ coincide at leading order in m_π^2. This is consistent with the result of the previous section that $T_2 = T(\mathbf{S})$ in the quenched approximation. This is because, in the quenched approximation, $f_\pi(N)$ is independent of N.

The leading order result $T(\mathbf{A}) = -T(\mathbf{S})$ shows that the attraction between pions in the representation **A** has the same strength as the repulsion in representation **S**. The reason for this is instructive. At leading order in the chiral expansion only tree diagrams with four-pion vertices contribute. There are various ways in which the flavor indices can be contracted, and Fig. 1 shows all the possibilities. The crucial observation is that the chiral Lagrangian (4.2) only contains terms with a single trace over flavor indices. Thus the direct and double-annihilation diagrams do not appear at leading order, for they have two flavor traces. Only the crossed and single-annihilation diagrams contribute. Since $T(\mathbf{S})$ is calculated from $D - C$, and $T(\mathbf{A})$ from $D + C$, if D vanishes we have $T(\mathbf{S}) = -T(\mathbf{A})$.

The higher order terms in Eqs. (4.3) come from $O(p^4, Mp^2, M^2)$ terms in the chiral Lagrangian, and from loop diagrams. Some of the contributions have two flavor traces [15], so that D does not vanish at non-leading order. This means that $T(\mathbf{A})$ and $T(\mathbf{S})$ will differ by terms of $O(m_\pi^2 \ln(m_\pi^2))$. Similarly, the higher order terms depend on the number of flavors, so $f_\pi^2 T_2$ and $f_\pi(N)^2 T(\mathbf{S})$ will also differ at $O(m_\pi^2 \ln(m_\pi^2))$ in the full theories.

The constraints of chiral symmetry are shown most clearly by the "gluon-exchange" and "quark-exchange" amplitudes. These result, respectively, from Figs. 1a and 1b

$$T_g = \tfrac{1}{2}\left(T(\mathbf{S}) + T(\mathbf{A})\right) = 0 + O(m_\pi^2 \ln(m_\pi^2))$$
$$T_q = \tfrac{1}{2}\left(T(\mathbf{S}) - T(\mathbf{A})\right) = \frac{1}{4f_\pi^2} + O(m_\pi^2 \ln(m_\pi^2)) \ . \qquad (4.4)$$

These are the amplitudes most directly related to the individual correlators we calculate on the lattice.

As we have seen, chiral symmetry places strong constraints on pion scattering amplitudes. In particular, the relativistically normalized amplitudes must vanish like m_π^2 at threshold, or equivalently, the non-relativistically normalized amplitudes must tend to a constant in the chiral limit. If one uses Wilson fermions on the lattice, however, chiral symmetry is broken at finite lattice spacing a. Thus the relativistically normalized amplitude will not vanish in the chiral limit, and T_{NR} will diverge proportional to a/m_π^2 [16]. This makes it difficult to extract the continuum amplitudes.

With staggered fermions, on the other hand, as long as one considers the scattering of the lattice pseudo-Goldstone pions, there are lattice Ward identities which constrain the lattice amplitudes. In fact, with certain assumptions concerning the smoothness of the amplitudes, and assuming that the pions dominate correlation functions for sufficiently small m_q, one can derive Eq. (4.3) on the lattice. The derivation, which extends the work of Ref. [11], is given in appendix B. It is valid in the quenched approximation as well as with dynamical quarks. It gives no information, however, on the $O(m_\pi^2 \ln(m_\pi^2))$ terms.

Staggered fermion scattering amplitudes involving non-Goldstone pions are not directly constrained by Ward identities. In general, these amplitudes should diverge in the chiral limit just as they do with Wilson fermions. The only difference is that the divergence should have a smaller coefficient: a^2/m_π^2 for staggered fermions rather than a/m_π^2. Thus a comparison of amplitudes for Goldstone and non-Goldstone pions provides a good test of staggered-flavor symmetry restoration.

5. Staggered complications

For Wilson fermions this completes the description of the calculation and the theoretical prelude. For staggered fermions there are, however, two further theoretical issues to be resolved. The first is that staggered fermions represent $N_f = 4$ degenerate flavors in the continuum limit, rather than a single fermion. The second is that the associated $SU(N_f)$ symmetry is broken at finite lattice spacing.

To resolve the problem of the extra flavors, we use essentially the same method as in calculations of weak matrix elements [11][17]. This approach is far from unique, but has the advantage of making maximal use of the softly broken axial symmetry, which is present with staggered fermions even for finite lattice spacing. Only for this method is the resulting scattering amplitude constrained by Ward Identities to have the same chiral limit as QCD.[4]

The method consists of three parts. The first is to introduce a separate staggered fermion field for each continuum quark. We use the notation of Ref. [19] and collect each staggered field into a matrix $Q_{\alpha a}$, where α is the usual spinor index, while $a = 1, 4$ is the staggered-flavor index. The upper case letters are a reminder that the field represents four flavors. Since four continuum quarks are required to define the correlators (see section 3), we need four staggered species, which we call U, D, S, and C. Thus our lattice theory has an $SU(4N_f)$ symmetry in the continuum limit, and is clearly different from the theory we want to study.

The second part of the method concerns the transcription of continuum pions onto the lattice. When we construct the correlators of Fig. 1, we must choose the staggered-flavor of the external pions. The pions are created by operators such as $\mathrm{Tr}(\overline{U}\gamma_5 D T_\eta)$, where the flavor is determined by T_η, which is one of the 16 Euclidean gamma matrices.[5] The rule is to always use the lattice pseudo-Goldstone pions, i.e. those having the flavor matrix T_5. This is the pion

[4] A review discussing these points in more detail is Ref. [18].

[5] More precisely, if $\eta = (\eta_1, \eta_2, \eta_3, \eta_4)$ is a vector of integers defined modulo 2, then $T_\eta = \gamma_1^{\eta_1}\gamma_2^{\eta_2}\gamma_3^{\eta_3}\gamma_4^{\eta_4}$. The γ_μ are hermitian, and $\gamma_5 = \gamma_1\gamma_2\gamma_3\gamma_4$.

whose mass vanishes in the limit $m \to 0$. We refer to pions having one of the 15 other staggered-flavors as non-Goldstone pions.

The final step is to remove overall factors of N_f in such a way that, in the continuum limit, the correlators we calculate are the same as those of QCD. In the problem at hand, we calculate Figs. 1a and 1b with external pions having flavor T_5. This means that the diagrams of Fig. 1 differ from their QCD counterparts by staggered-flavor factors. The direct diagram Fig. 1a has two flavor traces, and thus a flavor factor of $\left[\mathrm{Tr}(T_5^2)\right]^2 = N_f^2$. The crossed diagram Fig. 1b has a single flavor trace, so its flavor factor is $\mathrm{Tr}(T_5^4) = N_f$. To obtain results applicable to QCD we must divide by these factors. In the ratio $R(t)$, the denominator C_π^2 (Eq. (2.5)) has a flavor factor of N_f^2, since each pion propagator has a single flavor trace, $\mathrm{Tr}(T_5^2) = N_f$. Thus the staggered-flavor factors cancel in $D(t)$, while $C(t)$ must be corrected

$$C(t) = N_f C_{\mathrm{stagg}}(t) \ . \tag{5.1}$$

We use this definition in all of the following. It is for this definition of $C(t)$ that the analysis of appendix B applies.

This discussion does not address the extra factors of N_f in dynamical quark loops. What we have in mind is taking the appropriate root of the staggered fermion determinant so that, in the continuum limit, the same number of flavors flow around internal quark loops as in QCD. Then, at the level of diagrams, all contributions are exactly as in QCD.

A possible concern with this diagrammatic analysis is that the quantity we calculate, $R_2(t) = D_{\mathrm{stagg}} - N_f C_{\mathrm{stagg}}$, cannot be written as the correlator of a single product of operators, unlike the correlator we are aiming for, $C_{\pi\pi}$ (Eq. (2.3)). This is because we have multiplied different *contractions* by different factors. Thus $R_2(t)$ does not have a simple transfer matrix interpretation. We address this concern in appendix C.

We now turn to the second complication due to staggered fermions, that due to the breaking of the flavor symmetry at finite lattice spacing. At first sight, it would seem that this would simply introduce small corrections into the formulae used to extract the scattering amplitudes. These corrections would

presumably be proportional to a^2 [20]. It is true that we expect the scattering amplitude T to only receive small $O(a^2)$ corrections, but we do not directly calculate this amplitude. Instead, we calculate T indirectly from the energy shift δE, and it turns out that some of the flavor breaking corrections to the relation between T and δE are enhanced.

To see how these enhancements occur, we need to understand some details of the derivation of Eqs. (2.2) and (2.6), which we summarize as

$$R(t) \approx Z(1 - \delta E|t| + \tfrac{1}{2}\delta E^2 t^2) \ , \quad \delta E = \frac{T}{L^3}\left(1 + a_1\frac{T}{L} + a_2\frac{T^2}{L^2}\right) \ . \tag{5.2}$$

$R(t)$ is the quantity we actually calculate in order to extract T. A heuristic summary of the derivation is given in appendix A. The derivation proceeds by comparing the expansions of $R(t)$, δE and T in powers of the bare interaction. In particular, in the Euclidean evolution operator $R(t)$, the interaction causes the two pion system to jump between states in which the pions have different relative momenta, as shown in Eq. (A.9). Consequently, even if we project onto the state with zero relative momentum at initial and final times, the states at intermediate time can have either zero relative momentum (and thus be "on-shell") or non-zero relative momentum ("off-shell"). The interaction also mixes pairs of Goldstone pions with pairs of non-Goldstone pions. This means that pions with all 16 staggered-flavors appear at intermediate times, even if we project onto Goldstone pions at the initial and final times. As discussed in the appendix, Eq. (5.2) holds only when all pions are degenerate, and interact with equal strength.

At finite lattice spacing the pions are not degenerate, for the symmetry is broken down to a discrete subgroup[1] [21]. For example, the 16 pions created by the operators $\mathrm{Tr}(\overline{U}\gamma_5 D T_\eta)$, where T_η labels the possible gamma matrices, now fall into four 3-d and four 1-d representations, each having masses differing by $O(a^2)$. In the chiral limit, only the Goldstone pion ($T_\eta = T_5$) is massless, while at finite mass the Goldstone is lighter than the other pions. We denote a typical mass difference by δm_π.

The lack of degeneracy affects the on-shell intermediate states most severely. As discussed in appendix A, these states contribute in three ways

to Eq. (5.2). First, they lead to the terms of quadratic and higher order in t. One can think of the t^2 term as corresponding to two pions propagating freely except for two all-orders interactions of strength δE. To obtain the factor of $\frac{1}{2}t^2$, the state intermediate between the two interactions must be on-shell, i.e. degenerate with the external state of two Goldstone pions. If the intermediate state has an energy greater by $2\delta m_\pi$, there will be an extra exponential suppression, and $\frac{1}{2}t^2$ will be replaced by roughly

$$\begin{aligned}\int_0^t dt_1 \int_0^{t_1} dt_2 \; e^{-2\delta m_\pi (t_1 - t_2)} &= \frac{1}{(2\delta m_\pi)^2}\left(e^{-2\delta m_\pi t} - (1 - 2\delta m_\pi t)\right) \\ &\approx \tfrac{1}{2}t^2(1 - \tfrac{2}{3}\delta m_\pi t + \ldots) \; .\end{aligned} \tag{5.3}$$

We see here that the flavor breaking δm_π is enhanced by a factor of t. In our calculations $2\delta m_\pi \approx 0.1$ and we fit to times $t \approx 6-20$, so that $2\delta m_\pi t \approx 1$. Thus it is not legitimate to expand the exponential in the first line of Eq. (5.3), and the expected functional form is substantially changed from t^2. If one were to insist on fitting to t^2, the resulting coefficient would be substantially less than δE^2.

The second contribution of on-shell intermediate states is to terms proportional to tT^3/L^5 in $R(t)$, i.e. to the $1/L^2$ corrections to δE. Here also the flavor breaking is enhanced by factors of t, and the functional form will be roughly $(\exp(-2\delta m_\pi t)-1)/(2\delta m_\pi)$ instead of linear in t. Thus the value of δE extracted from a linear fit will be incorrect at the level of $1/L^2$ corrections.

The final contribution of on-shell intermediate states is to the parts of Z proportional to $1/L^2$. An error here also affects the $1/L^2$ corrections to δE.

The effect of flavor breaking is less important for off-shell intermediate states. This is because the splitting between the discrete energies allowed by the finite box is larger than δm_π. The condition for this is

$$\sqrt{m_\pi^2 + \left(\frac{2\pi}{L}\right)^2} - m_\pi > \delta m_\pi \; , \tag{5.4}$$

and this is satisfied in our calculations. Clearly for large enough L, at fixed a, this condition will not be satisfied. In this case, the derivation of the $1/L^4$ term in δE is not valid, because the lower limit on the momentum sums for non-Goldstone off-shell intermediate states becomes $\sim \delta m_\pi$ and not $\sim \pi/L$. In this limit, only the leading order term in δE can be used.

In summary, for our calculation we can use Eq. (5.2) to extract T as long we work in a regime where (i) only the constant and linear terms in t are needed to describe $R(t)$; and (ii) L is large enough that we need not rely on the $1/L^5$ term in δE. The resulting T should have errors of $O(a^2)$ and of $O(1/L^2)$.

We stress that the failure of the $1/L^5$ terms in Eq. (5.2) is due to the fact that we are trying to apply Lüscher's formula to a situation for which it was not derived. The formula applies to finite volume energy shifts, are we are *not* calculating such a shift. Instead we are calculating the coefficient of the term linear in t. In fact, if we did calculate the long time exponential behavior of the correlator, we could use Lüscher's formula to extract a lattice Goldstone pion scattering amplitude. It is clear from the above analysis, however, that it would have no relation with the continuum amplitude we are seeking to extract. In fact, it is probable that it would have the opposite sign from the continuum amplitude, since the lightest state would likely be lighter than $2m_\pi$.

6. Method of calculation

There is one more obstacle that must be overcome with staggered fermions. In the previous section we discussed how to extract scattering amplitudes using correlators in which the initial and final operators coupled only to pairs of Goldstone pions. One is forced to rely on the terms in $R(t)$ constant and linear in t, since quadratic and higher order terms are affected by staggered-flavor breaking. Any coupling of the initial and final operators to non-Goldstone pions would contaminate the linear term itself, and thus complicate the analysis. It turns out that with the propagators available from spectrum calculations, such contamination is unavoidable.

The problem stems from the form of the operators with which we create the two pion state in the correlator $C_{\pi\pi}$. These are denoted $\mathcal{S}_3$ and $\mathcal{S}_4$ in Eq. (2.3). Ideally, we would like to use $\mathcal{S}(t) = \sum_{\vec{x}} \mathcal{O}(\vec{x}, t)$, where $\mathcal{O}$ is a local

pion operator, but this is not practical as it would require propagators starting from all points on a timeslice. Instead, in our calculation $\mathcal{S}$ is the product of a wall-source for the quark with a wall-source for the antiquark:

$$\mathcal{S}(t) = \sum_{\vec{x}} \mathcal{A}'(\vec{x})\overline{\chi}(\vec{x},t)_a \sum_{\vec{y}} \mathcal{A}(\vec{y})\chi(\vec{y},t)_a \ . \tag{6.1}$$

Here χ is the one-component staggered fermion, with color index a, and we have suppressed the flavor indices. The phases $\mathcal{A}$ and $\mathcal{A}'$ determine the staggered-flavor of the source, and will be discussed shortly. This source has the advantage of coupling only to zero momentum pions, and thus works well for pion two-point functions. The problem arises when there are two such sources on a single timeslice, for then there are contributions in which the quarks and antiquarks bind together to form pions in the opposite way to that we impose by the contraction of color indices. These "Fierz" contributions are not suppressed by powers of $1/L$, and couple to pairs of both Goldstone and non-Goldstone pions.

The effect of these contributions is that the lattice correlator which one might think to be the direct diagram actually contains a component of the crossed diagram, and vice versa. This is not important for Wilson fermions as long as one calculates $D(t) \mp C(t)$, for these combinations project the Fierz contributions onto the desired flavor. The only effect is that the overall constant $Z_{\pi\pi}/Z_\pi^2$ may differ from unity by terms of $O(1)$ rather than $O(1/L^2)$. The Fierz contributions are, however, a problem with staggered fermions. This is because, as mentioned above, they introduce large flavor breaking into the linear terms in $R(t)$. In addition, it turns out with our wall sources that the combinations $D \mp C$ do not project onto representations of the $SU(4N_f)$ symmetry group, even in the continuum limit.

There are also Fierz terms from the operators which destroy the two pions. Here, however, the operator used in the calculation does consist of the product of two $\vec{p} = 0$ pions instead of quark sources. This means that the Fierz terms are small, since they require the two particles to overlap. Naively these terms are $O(1/L^3)$, though, like the wavefunction renormalization, they are likely to be in fact of $O(1/L^2)$. If so, they will affect the scattering amplitudes at the

level of $1/L^2$ corrections. Since this is the level at which the amplitudes are already uncertain, these Fierz contributions from the final operators can be ignored.

To understand how we address the problem of Fierz contributions we must first explain our sources in more detail. We follow the notation of Ref. [22], which also contains a more complete discussion of our wall sources. The phases in Eq. (6.1) depend only on the values of $\vec{x}$ modulo 2, i.e., if we write $\vec{x} = 2\vec{y}+\vec{\eta}$, then $\mathcal{A}(\vec{x}) = \mathcal{A}(\vec{\eta})$. We use two types of source, q and o. Choosing $t = 0$ to simplify the notation, these are

$$\begin{aligned} q_a &= \sum_{\vec{x}} \chi(\vec{x})_a \ ; \qquad \overline{q}_a = \sum_{\vec{x}} (-1)^{\eta_x+\eta_y+\eta_z} \overline{\chi}(\vec{x})_a \\ o_a &= \sum_{\vec{x}} (-1)^{\eta_x+\eta_y+\eta_z} \chi(\vec{x})_a \ ; \qquad \overline{o}_a = \sum_{\vec{x}} \overline{\chi}(\vec{x})_a \ . \end{aligned} \tag{6.2}$$

These sources are made gauge invariant by fixing the source timeslice to Coulomb gauge. Combining these sources we can create four different pions: the Goldstone pion π (with flavor T_5) and the non-Goldstones π_3, $\widetilde{\pi}$ and $\widetilde{\pi}_3$, with flavor T_3T_5, T_4T_5 and $T_3T_4T_5$ respectively

$$\begin{aligned} \mathcal{S}(\pi) &= \sum_a \overline{q}_a q_a + \overline{o}_a o_a \\ \mathcal{S}(\pi_3) &= \sum_a \overline{q}_a q_a - \overline{o}_a o_a \\ \mathcal{S}(\widetilde{\pi}) &= \sum_a \overline{q}_a o_a + \overline{o}_a q_a \\ \mathcal{S}(\widetilde{\pi}_3) &= \sum_a \overline{q}_a o_a - \overline{o}_a q_a \ . \end{aligned} \tag{6.3}$$

In $C_{\pi\pi}$ we place two such operators on a single timeslice, i.e. $\mathcal{S}(\pi)\mathcal{S}(\pi)$. We want to rewrite this product operator in a basis in which, say, the quarks from the two operators are interchanged. To do this we rearrange the colors using

$$\delta_{ab}\delta_{cd} = \tfrac{1}{3}\delta_{ad}\delta_{cb} + 2\sum_{i=1}^{8} T^i_{ad}T^i_{cb} \ . \tag{6.4}$$

Thus the color Fierz gives a factor of $\frac{1}{3}$.[6] We also need the staggered-flavor Fierz rearrangement formula, and it straightforward to show that

$$\mathcal{S}(\pi)\mathcal{S}(\pi) \to \tfrac{1}{2}\left(\mathcal{S}(\pi)\mathcal{S}(\pi) + \mathcal{S}(\pi_3)\mathcal{S}(\pi_3) + \mathcal{S}(\widetilde{\pi})\mathcal{S}(\widetilde{\pi}) - \mathcal{S}(\widetilde{\pi}_3)\mathcal{S}(\widetilde{\pi}_3)\right) , \quad (6.5)$$

where we have omitted the color indices. Thus the source which naively creates two Goldstone pions, also couples to $\pi\pi$, $\pi_3\pi_3$, $\widetilde{\pi}\widetilde{\pi}$ and $-\widetilde{\pi}_3\widetilde{\pi}_3$ with the quarks and antiquarks combined in the "wrong" way. The relative strength of these couplings is $\frac{1}{6}$: $\frac{1}{3}$ from the color Fierz multiplied by $\frac{1}{2}$ from the staggered-flavor Fierz. Note that there is no possibility of double counting here as each of the staggered fermions has a different flavor under the overall $SU(4)$ symmetry, so the pions resulting from "right" and "wrong" $\overline{\chi}\chi$ combinations have different flavors.

The Fierz contributions force us to face head on the problem of staggered-flavor symmetry breaking. To do this, it is simplest to consider $D(t)$ and $C(t)$ separately. We break down both into a part without Fierz terms, and the contribution from Fierz terms, e.g. $D = D_0 + D_{\rm Fierz}$. We know from the previous sections how D_0 and C_0 are related to the scattering amplitudes. For $D_{\rm Fierz}$ and $C_{\rm Fierz}$ we use the understanding developed in appendix A to take out explicitly all the terms in which corrections due to flavor symmetry breaking are enhanced. The remaining corrections are of the same size as the uncertainties in the formulae for D_0 and C_0, i.e. of $O(a^2)$ and $O(1/L^2)$.

The expressions for D_0 and C_0 can be obtained by combining Eqs. (2.2), (2.7) and (4.4)

$$\begin{aligned} D_0(t) &= 1 + O(1/L^2) - t\left(\frac{T_g}{L^3} - \frac{c_1 m_\pi (T_g^2 + T_q^2)}{4\pi L^4} + O(1/L^5)\right) + O(t^2) \\ C_0(t) &= O(1/L^2) + t\left(\frac{T_q}{L^3} - \frac{c_1 m_\pi (2T_g T_q)}{4\pi L^4} + O(1/L^5)\right) + O(t^2) \ . \end{aligned} \quad (6.6)$$

[6] We ignore the part of the rearranged operator consisting of two color octet pions, for neither operator couples to physical states. There may be some coupling of the two octet operator to two physical pions, but this involves an overlap factor which contributes to δE at $O(1/L^5)$, the level at which Eq. (2.2) is unreliable.

We have assumed that $Z_{\pi\pi}/Z_\pi^2 - 1 = O(1/L^2)$ for both the S and A representations. This is true for local zero-momentum sources (as discussed in appendix A), but is an assumption, albeit reasonable, for our wall sources. To give us some idea of how good this assumption is, we multiply both D and C by a factor of Z in our fits. A consistency check is then that Z comes out to be close to unity.

We now consider the Fierz contribution to D. In this contribution, the initial pions produced by the Fierzed source must interact by quark exchange in order to couple to the final operators. As shown in Eq. (6.5), the initial pions can be either Goldstone pions or non-Goldstone pions. If they are Goldstone pions, the Fierz term is just like the correlator C_0 in Eq. (6.6). Aside from small corrections, C_O is proportional to t, and one can think of this as coming from two pions propagating freely except for an interaction which can take place at any time. For initial non-Goldstone pions, the physical picture is similar: the non-Goldstone pair propagates for a time t' and then scatters into the Goldstone pair, which propagates for the remaining time. We must take into account, however, the difference between the Goldstone and non-Goldstone pion masses. We do this with the replacement

$$t = \sum_{t'=1}^{t} 1 \longrightarrow H(t) = \sum_{t'=1}^{t} \exp(-2\delta m_\pi t') \ . \quad (6.7)$$

Note that when $\delta m_\pi \to 0$, $H(t) \to t$. As Eq. (6.5) shows, the Fierzed source produces three types of non-Goldstone pions. We use a common δm_π for all three, since, within our errors, they are degenerate [22].

As discussed above, the source produces each of these pion pairs with an overall factor of $\frac{1}{6}$. This will receive corrections at $O(1/L^2)$, and so, in our fits, we parameterize the strength of the Fierz amplitude by F. A consistency check is then that we find $F \approx \frac{1}{6}$.

We also need to calculate the sign of the contributions of the four different pion pairs. This is a combination of the sign from the flavor Fierz transformation given in Eq. (6.5), and the staggered-flavor factor multiplying the scattering amplitude. For initial pions of flavor T_η, the latter factor is $\mathrm{Tr}(T_5 T_\eta T_5 T_\eta)/N_f$.

For π, π_3 and $\widetilde{\pi}$ pairs this is $+1$, while for $\widetilde{\pi}_3$ pairs it is -1. These signs cancel those in Eq. (6.5), with the result that all four pion pairs contribute with the same sign.

We must also account for the fact that $C_0(t)$ contains an overall factor of N_f which is included by hand, Eq. (5.1). The Fierz contributions to $D(t)$ do not contain this factor, and thus, when related to $C_0(t)$, must be multiplied by $1/N_f$. Putting all this together, we have

$$D_{\rm Fierz}(t) \approx \frac{F}{N_f} C_0(t)(1+3H(t)/t) \approx F\frac{(t+3H(t))Q}{L^3} \ . \tag{6.8}$$

Here we have introduced the notation

$$N_f Q = T_q - 2T_q T_g c_1 m_\pi/(4\pi L) + O(1/L^2) \ . \tag{6.9}$$

The analysis is simpler for $C(t)$. The Goldstone pion pair produced by the Fierz rearranged wall sources can propagate without scattering, or undergoing a gluon exchange, before being destroyed. The scattering of the non-Goldstone pairs into a Goldstone pair by gluon exchange vanishes in the continuum limit, since the staggered-flavor traces vanish. Ignore this small contribution

$$\begin{aligned} C_{\rm Fierz}(t) &\approx N_f F D_0(t) \approx N_f F(1-tG/L^3) \ , \\ G &= T_g - (T_g^2+T_q^2)c_1 m_\pi/(4\pi L) + O(1/L^2) \ . \end{aligned} \tag{6.10}$$

The factor of N_f is the overall factor included by hand in the definition of C.

In addition to the correlators in which we both create and destroy the fields with Goldstone pion operators, we also calculate with sources and/or sinks creating a $\pi_3\pi_3$ pair. This allows us to test our parameterizations of the Fierz terms, and to study flavor symmetry breaking in the scattering amplitude. The correlators we calculate are (cf. Eq. (2.3))

$$\begin{aligned} \pi\pi \to \pi\pi : &\quad \langle \pi(t)\pi(t)\mathcal{S}(\pi)\mathcal{S}(\pi)\rangle / \langle \pi(t)\mathcal{S}(\pi)\rangle^2 \ , \\ \pi\pi \to \pi_3\pi_3 : &\quad \langle \pi_3(t)\pi_3(t)\mathcal{S}(\pi)\mathcal{S}(\pi)\rangle / \langle \pi(t)\mathcal{S}(\pi)\rangle^2 \ , \\ \pi_3\pi_3 \to \pi\pi : &\quad \langle \pi(t)\pi(t)\mathcal{S}(\pi_3)\mathcal{S}(\pi_3)\rangle / \langle \pi(t)\mathcal{S}(\pi)\rangle^2 \ , \\ \pi_3\pi_3 \to \pi_3\pi_3 : &\quad \langle \pi_3(t)\pi_3(t)\mathcal{S}(\pi_3)\mathcal{S}(\pi_3)\rangle / \langle \pi_3(t)\mathcal{S}(\pi_3)\rangle^2 \ . \end{aligned} \tag{6.11}$$

For each of these, we calculate both the direct and crossed correlators. Notice that our notation has the flavor of the wall sources appearing first (to the left of the arrow).

Extending the analysis given above, we find, using the flavor Fierz

$$\mathcal{S}(\pi_3)\mathcal{S}(\pi_3) \to \tfrac{1}{2}\left(\mathcal{S}(\pi)\mathcal{S}(\pi) + \mathcal{S}(\pi_3)\mathcal{S}(\pi_3) - \mathcal{S}(\widetilde{\pi})\mathcal{S}(\widetilde{\pi}) + \mathcal{S}(\widetilde{\pi}_3)\mathcal{S}(\widetilde{\pi}_3)\right) \ , \tag{6.12}$$

that (we include the $\pi\pi \to \pi\pi$ formulae for completeness)

$$\begin{aligned} \pi\pi \to \pi\pi : &\quad D(t) = Z(1-tG/L^3) + F(t+3H(t))Q/L^3 \\ &\quad C_{\rm stagg}(t) = ZtQ/L^3 + F(1-tG/L^3) \\ \pi\pi \to \pi_3\pi_3 : &\quad D(t) = F\left(-te^{-2\delta m_\pi t} + H(t)\right)Q/L^3 \\ &\quad C_{\rm stagg}(t) = ZH(t)Q/L^3 + Fe^{-2\delta m_\pi t}(1-tG/L^3) \\ \pi_3\pi_3 \to \pi\pi : &\quad D(t) = F(t-H(t))Q/L^3 \\ &\quad C_{\rm stagg}(t) = ZH(t)Q/L^3 + F(1-tG/L^3) \\ \pi_3\pi_3 \to \pi_3\pi_3 : &\quad D(t) = Z(1-tG/L^3) + F(H'(t)+3t)Q/L^3 \\ &\quad C_{\rm stagg}(t) = ZtQ/L^3 + F(1-tG/L^3) \ , \end{aligned} \tag{6.13}$$

where

$$H'(t) = \sum_{t'=1}^{t} e^{2\delta m_\pi t'} \ . \tag{6.14}$$

We express the results in terms of $C_{\rm stagg} = C/N_f$, since this is the correlator we actually calculate.

These are the equations with which we compare our numerical results. We do so in the region where t is both large enough that contributions from excited states (which are not included in the equations) have died away, and small enough that terms quadratic in t are small. From this comparison we can extract G and Q, which, according to Eqs. (6.9) and (6.10), should reach finite limits as $L \to \infty$, with known $1/L$ corrections.

Two of the correlators involving π_3 are particularly interesting. The first is $C(t : \pi_3\pi_3 \to \pi\pi)$, which differs from $C(t : \pi\pi \to \pi\pi)$ only by the replacement $t \to H(t)$ in the first term. Comparison of these two correlators is thus a good

TABLE 1. Lattices and propagators used in numerical calculations.

β	a^{-1}(GeV)	Size	Sample *	m_q
5.7	1.0	$16^3 \times 32$	12+15	0.005, 0.01, 0.015
5.7	1.0	$16^3 \times 32$	13	0.03, 0.06, 0.09
6.0	2.0	$16^3 \times 40$	18+13	0.01, 0.02, 0.03
6.0	2.0	$24^3 \times 40$	15	0.01, 0.02, 0.03

* *The number of lattices in each independent stream is given.*

way of testing the form of $H(t)$. Second, $C(t : \pi_3\pi_3 \to \pi_3\pi_3)$ should be the same as $C(t : \pi\pi \to \pi\pi)$. That this is so tests the size of $O(a^2)$ corrections, which have been ignored in this parameterization.

We close this section with a note on the calculation using Wilson fermions. The first two lines of Eq. (6.13) apply to Wilson fermions if one sets $N_f = 1$ and $H(t) = 0$. One sees explicitly that if one forms $D \mp C$, the Z and F terms combine into the leading terms of pure exponentials. It is also clear, however, that if one only has a calculation of $D(t)$, and does not know F, one cannot extract $T_2 = T_g - T_q$. This is the case in the calculation of Ref. [12], where the use of a smeared source prohibits estimation of F.

7. Numerical results

We calculate the correlators of Eq. (6.13) on the quenched lattices and using the quark masses listed in Table 1. We also give the nominal values of a^{-1} which we use to convert to physical units when needed. The two lattices at $\beta = 6$ are the most important for our study, as they allow a direct calculation of any finite volume dependence. The quark masses are moderately small, roughly $1.5m_s$, m_s and $0.5m_s$, where m_s is the physical strange quark mass [22]. Unlike the lattices at $\beta = 6$, which are on the edge of the scaling region, those at $\beta = 5.7$ are definitely outside this region. Nevertheless, the lattices are of interest because, in addition to quarks of mass similar to those at $\beta = 6$, we also use considerably smaller quark masses. These are roughly $6\overline{m}$, $4\overline{m}$ and $2\overline{m}$, where $\overline{m} = (m_u + m_d)/2$, m_u and m_d being the physical up and down quark masses.

Complete details of the lattice generation and propagator calculations are given in Ref. [22], and we mention only the pertinent features. All propagators are calculated with Dirichlet boundary conditions in the time direction, with the wall sources placed on one of the boundary timeslices. The propagators thus fall off over the entire time extent of the lattice, distorted only by boundary reflections. The "local" pion operators ($\mathcal{O}_1$ and $\mathcal{O}_2$ in Eq. (2.3)) are actually smeared out over a 2^4 hypercube. In the notation of Ref. [22], the operator for the Goldstone π is $\gamma_4\gamma_5 \otimes \gamma_5$, while that for the non-Goldstone π_3 is $\gamma_5 \otimes \gamma_3\gamma_4\gamma_5$. We prefer these to single timeslice operators, as they couple less strongly to the excited states in their respective channels [23].

In Ref. [22] we studied the finite size dependence of pion masses and decay constants on the lattices at $\beta = 6$. Such dependence comes from chiral loops and from glueball exchange, the corrections falling as $\exp(-m_\pi L)$ and $\exp(-m_G L)$, respectively, m_G being the glueball mass. These exponentially falling corrections must be negligible if we are to extract finite size effects which fall as powers of $1/L$. We found that finite size effects in m_π, f_π and m_{π_3} are smaller than the statistical errors. For m_π these errors are $\sim 2\%$, while for the other quantities they are somewhat larger. We conclude that the lattices are large enough to attempt a calculation of the scattering amplitude.

TABLE 2. Parameters used in fitting at $\beta = 5.7$.

m_q	m_π	m_{π_3}	f_π
0.090	0.789	1.11	0.196(9)
0.060	0.659	0.99	0.171(6)
0.030	0.482	0.82	0.142(4)
0.015	0.350	0.71	0.133(4)
0.010	0.289	0.66	0.127(5)
0.005	0.208	0.61	0.124(6)

The parameterizations we use to fit the correlators (Eq. (6.13)) require as inputs the differences between the mass of the Goldstone π and those of

the π_3, $\widetilde{\pi}$ and $\widetilde{\pi}_3$. At $\beta = 5.7$ flavor symmetry is badly broken, and the non-Goldstone pions are considerably heavier [22]. This is illustrated by the results for m_π and m_{π_3} given in Table 2. It turns out that, because of this large mass difference, the non-Goldstone contribution to the $\pi\pi \to \pi\pi$ correlators is negligible. Furthermore, the signal is poor in the correlators involving $\pi_3\pi_3$, so we only have results for the $\pi\pi \to \pi\pi$ correlators.

In Table 3 we give the results for m_π and m_{π_3} from the 24^3 lattices at $\beta = 6$ [22]. Here the flavor symmetry is less badly broken, and there are reasonable signals in all the correlators of Eq. (6.13). Within errors, the π_3, $\widetilde{\pi}$ and $\widetilde{\pi}_3$ are degenerate, and, for simplicity, we assume exact degeneracy, taking the π_3 mass for all three. We do not include errors in these masses in the following analysis, as these errors are smaller than the other uncertainties.

TABLE 3. Parameters used in fitting at $\beta = 6$.

m_q	m_π	m_{π_3}	f_π	$R_{\rm wall}(24^3)$	$R_{\rm wall}(16^3)$
0.03	0.417	0.461	0.069(6)	0.83	0.97
0.02	0.338	0.386	0.063(5)	0.76	0.96
0.01	0.238	0.288	0.059(4)	0.84	1.1

Tables 2 and 3 also include the values for f_π extracted in Ref. [22]. (The results for the larger three masses at $\beta = 5.7$ are new.) These are needed to compare the scattering amplitudes we extract to the current algebra predictions.

To arrive at the parameterizations of Eq. (6.13) we assume that flavor symmetry breaking is small in quantities other than the pion masses. In particular, we assume that the amplitudes for the wall sources to create pions, the amplitudes for the operators to destroy the pions, and the scattering amplitudes from two pions to two other pions are all independent of flavor. This is true in the continuum limit, but there are corrections of $O(g^2)$ and $O(a^2)$. To give an idea of how large these corrections are we include in Table 3 results for the following ratio of amplitudes (using the notation of Ref. [22]):

$$R_{\rm wall} = \frac{\mathcal{A}_{\rm wall}(\pi)}{\mathcal{A}_{\rm wall}(\pi_3)};\ \mathcal{A}_{\rm wall}(\pi) = \langle\pi|qq + oo|W\rangle,\ \mathcal{A}_{\rm wall}(\pi_3) = \langle\pi_3|qq - oo|W\rangle\ . \tag{7.1}$$

Here W represents the complicated state that the wall operator acts upon, and q and o are the two types of wall source. This ratio gives the relative strength of the π and π_3 walls. The statistical errors in these amplitudes are $\sim 15\%$, and within these errors the ratio is consistent with unity. Since the non-Goldstone contribution is a relatively small correction for the main correlators of interest, the approximation of assuming equal amplitudes is adequate.

We now turn to our results, beginning with the crossed $\pi\pi \to \pi\pi$ correlator, $C(t)$. This is the correlator with the best signal and the simplest interpretation. According to Eq. (6.13), it should have a non-zero intercept of $F \sim 1/6$ and a linear dependence on t, with a slope which should vanish as $1/L^3$. The slope should be dominated by the quark exchange amplitude, as the gluon exchange amplitude is suppressed by the Fierz factor F. The results for $C_{\rm stagg}(t) = C(t)/N_f$ are shown in Figs. 2a-c. The errors on the points are statistical, determined by single-elimination jackknife. The results are in good agreement with our expectations. All graphs show an intercept close to 1/6, and a clear linear behavior. At $\beta = 6$, the slope is much greater on the 16^3 than on the 24^3 lattices. There are boundary effects at large times, beginning $8 - 10$ timeslices from the end of the lattice, as is most evident at $\beta = 5.7$. For small t, however, there is little sign of boundary effects, the linear behavior beginning almost immediately.

In order to extract G and Q, we need to combine the results for $C(t)$ with those from the direct correlator $D(t)$. This is expected to have an intercept of $Z \sim 1$, and a linear term in which the quark exchange amplitude is suppressed by F compared to the gluon exchange amplitude. It turns out that in our data the contributions of these two amplitudes to the slope are similar. At $\beta = 6$, the analysis is complicated by the presence of the non-Goldstone pion contribution, *i.e.* the term proportional to $H(t)$ in Eq. (6.13). (At $\beta = 5.7$ the non-Goldstone pions are too heavy to contribute.) This introduces a small curvature in $D(t)$. The results are displayed in Figs. 3a-c, using vertical offsets to separate the data for different masses. Accounting for these offsets, we see that the intercepts lie close to the expected value. The errors are larger than those for $C(t)$, and the linear behavior is less clean. There is some evidence

for the expected curvature at $\beta = 6$, but the errors are too large for this to be convincing.

To extract Z, F, G and Q we must simultaneously fit $C(t)$ and $D(t)$ to the forms in Eq. (6.13). To do this we make two simplifications. First, we ignore correlations when doing the fitting, so that we do not have a quantitative measure of the goodness of fit. This simplification is made of necessity, as we do not have enough configurations to calculate the full correlation matrix for the values of C and D to which we fit. We can, however, calculate the errors in the parameters of the fit, using single-elimination jackknife. (There are actually two measurements on each configuration, one with the wall source at each end, but we average these together and count them as a single measurement in the jackknife calculations.) The second simplification is to approximate $H(t)$ by a linear function within our chosen time range. This simplifies fitting, and is a good approximation.

To apply this method we must choose a time range, $t_{\rm min} - t_{\rm max}$. This must be done so as to avoid possible contamination from boundary effects and from t^2 terms. As is most clear in $C(t)$ at $\beta = 5.7$ (Fig. 2a), boundary effects cause the slope to increase at large t. Because of this, as one increases $t_{\rm max}$, the slope increases monotonically, and there is no stable asymptotic result. The same problem would be caused by t^2 terms. What we do in practice is to look for a set of reasonable time ranges for which the results are consistent within the errors. We consider values for $t_{\rm min}$ down to 6, and $t_{\rm max}$ up to 28. To give an idea of the sensitivity to time range we give the results from the fits to $t = 6-16$ and $t = 10-20$ in Tables 4 and 5. In addition, Figures 2 and 3 show the fits for $t = 6-16$, and their extensions outside the fitting range.

Table 4 shows that Z and F are only sensitive to the time range for the $L = 16$ lattice at $\beta = 6$, although even on this lattice the changes are of marginal significance. This lattice has the smallest physical size, so that, at a given pion mass, the finite volume effects are largest. In particular this means that the t^2 terms are largest, so that we expect the greatest sensitivity to changes in the time range. The results show that $\delta Z = Z - 1$ and $\delta F = F - \frac{1}{6}$ are both small. This confirms the assumption made in the previous section that the

TABLE 4. Results for Z and F.

	$t = 6-16$		$t = 10-20$	
m_q	Z	F	Z	F
$\beta = 5.7$, $16^3 \times 32$				
0.090	1.001(1)	0.1675(3)	1.000(1)	0.167(1)
0.060	1.002(1)	0.1680(4)	1.000(1)	0.168(1)
0.030	1.004(2)	0.1694(6)	1.002(1)	0.168(1)
0.015	1.004(1)	0.173(1)	1.002(1)	0.173(1)
0.010	1.005(1)	0.177(1)	1.003(2)	0.177(1)
0.005	1.007(2)	0.186(1)	1.008(2)	0.185(2)
$\beta = 6$, $16^3 \times 40$				
0.03	1.004(8)	0.172(4)	0.983(19)	0.166(7)
0.02	1.014(7)	0.181(3)	0.990(16)	0.172(5)
0.01	1.026(10)	0.196(4)	0.994(15)	0.186(6)
$\beta = 6$, $24^3 \times 40$				
0.03	1.004(3)	0.167(1)	1.004(5)	0.167(1)
0.02	1.007(4)	0.168(1)	1.006(6)	0.168(2)
0.01	1.012(6)	0.174(1)	1.010(7)	0.175(2)

$Z_{\pi\pi}/Z_\pi^2$ is close to unity even for wall sources. We also suggested that δZ and δF should be proportional to $1/L^2$. If so, we would expect that $\delta Z(L = 16)/\delta Z(L = 24) \approx \delta F(L = 16)/\delta F(L = 24) \approx 2$. Only δF is statistically significant, and we do find that $\delta F(L = 16)$ is larger than $\delta F(L = 24)$, the ratio even being consistent with the expected factor of 2, modulo the usual systematic and statistical uncertainties.

As shown in Table 5, Q and G are more sensitive to the fitting range. We draw the following conclusions from the results:

1. For $\beta = 5.7$, $L = 16$, the results do not depend on the time range: Q and G agree for the two fits within errors. Q is well determined, while G is consistent with zero.
2. The same is true on the large lattice ($L = 24$) at $\beta = 6$. Indeed, if we extend the fitting range to $t = 10-28$, we find no significant changes in the parameters.

TABLE 5. Results for Q and G.

		$t = 6-16$		$t = 10-20$	
m_q	$1/(16f_\pi^2)$	Q	G	Q	G
$\beta = 5.7$, $16^3 \times 32$					
0.090	1.64(16)	1.7(1)	-0.3(2)	1.7(2)	-0.6(3)
0.060	2.15(16)	2.2(2)	-0.2(4)	2.1(3)	-0.6(6)
0.030	3.1(2)	3.2(4)	0.0(5)	3.5(5)	-0.5(7)
0.015	3.5(2)	3.6(3)	-0.2(4)	3.7(3)	-0.6(4)
0.010	3.9(3)	3.9(3)	-0.2(4)	3.9(4)	-0.7(4)
0.005	4.1(4)	4.2(4)	-0.5(5)	4.5(6)	-0.1(4)
$\beta = 6$, $16^3 \times 40$					
0.03	13.1(2.3)	14.6(1.6)	-10(4)	16.1(2.6)	-17(7)
0.02	15.8(2.5)	15.8(1.4)	-7(4)	17.6(1.4)	-15(7)
0.01	18.0(2.4)	19.6(1.4)	-7(5)	21.5(1.4)	-17(7)
$\beta = 6$, $24^3 \times 40$					
0.03	13.1(2.3)	13.2(1.1)	- 8(6)	13.7(1.3)	-8(5)
0.02	15.8(2.5)	16.1(1.6)	-5(6)	16.0(1.7)	-6(5)
0.01	18.0(2.4)	19.3(2.2)	-1(7)	17.2(2.1)	-4(5)

3. The same is not true on the $\beta = 6$, $L = 16$ lattices. There is a systematic increase in Q and $|G|$ when going from $t = 6-16$ to $t = 10-20$. The results for $t = 10-28$ are larger still. On the other hand, using $t = 6-12$ gives almost the same results for Q as for $t = 6-16$, while for G we find the smaller results $-8(4)$, $-5(3)$ and $-4(5)$ for $m_q = 0.03$, 0.02 and 0.01 respectively. We conclude that we must use $t_{\max} \leq 16$, and that only the results for Q are reliable.

Based on this analysis we consider $t = 6-16$ to be a reliable range for extracting Q for all three lattices, and we use this range in the following. We cannot, however, extract G, although we can roughly bound it.

Before proceeding to the analysis of the results for Q and G, we consider whether the restriction $t_{\max} \leq 16$ on the $\beta = 6$, $L = 16$ lattices could be due to t^2 terms, or whether instead it is due mainly to other effects such as boundary reflections. The data themselves suggest the latter interpretation, since Figs.

2b and 3b show more of a kink than a smooth quadratic form. We can make a crude estimate of the expected size of t^2 terms by ignoring Fierz contributions. Then it follows from Eqs. (2.6) and (4.4) that

$$C_{\text{stagg}}(t) = \frac{tQ}{L^3} - \frac{t^2QG}{L^6} + O(t^3) \,,$$
$$D(t) = 1 - \frac{tG}{L^3} + \frac{t^2(G^2 + N_f^2Q^2)}{2L^6} + O(t^3) \,. \tag{7.2}$$

The effect of flavor breaking is effectively to reduce the coefficient of t^2 so these equations overestimate the expected effect. Consider first the crossed amplitude. The leading correction comes from an additional gluon exchange, and has relative size $-tG/L^3$. Since G is negative, the t^2 term is positive, and this is consistent with the curvature we find for $C(t)$. The magnitude of the t^2 term is, however, too small to explain the curvature. To see this, we use the largest values of $|G|$ which we find, and compare the t^2 term predicted by Eq. (7.2) to the size of the errors in $C(t)$. At $\beta = 5.7$, taking $-G < 0.5$, the t^2 term is less than 7% of the error for all t. At $\beta = 6$, with $G = -10$, the t^2 term is about one third of the error for $t > 20$, for both $L = 16$ and $L = 24$. Since the deviation from the fit for $L = 16$ (Fig. 2b) is about the same as the error for $t > 20$, this suggests that no more than a third of the curvature can be explained by t^2 terms.

For the direct amplitude the t^2 terms are potentially larger because of the factor of N_f^2 multiplying Q^2. This enhancement comes from the fact that if there are two quark exchanges the intermediate pions can have any staggered-flavor. Since the non-Goldstone pions are heavier, however, this enhancement factor will be reduced. Indeed for $\beta = 5.7$ we expect the "effective" N_f^2 to be close to 1, in which case the t^2 term turns out to be $< 10\%$ of the error in D for all t, and thus negligible. For $\beta = 6$, the effective N_f^2 will be larger. If we assume that it is ~ 8, then the t^2 terms are no larger than one third of the error in D for $L = 24$. For $L = 16$, however, they are similar in magnitude to the error in D for $t > 20$. Since the deviations from linearity are similar to the errors, it is possible that the t^2 terms are the dominant source of curvature.

The final step in the analysis is to extract T_q and T_g. Recall that

$$N_f Q = T_q - 2T_q T_g \frac{c_1 m_\pi}{4\pi L} + O(1/L^2) ,$$
$$G = T_g - (T_g^2 + T_q^2)\frac{c_1 m_\pi}{4\pi L} + O(1/L^2) , \tag{7.3}$$

so, in principle, we can solve these equations given Q and G. This is not possible, however, in practice. The errors on G are too large, and (as we discuss below) the convergence of the $1/L$ expansion for G too poor. Instead, at $\beta = 6$, we can plot Q versus m_π/L and try and extrapolate to $L = \infty$. This is to be done separately for each quark mass. The results from Table 5 (using $t = 6 - 16$) are collected in Fig. 4. (Recall that there is no correlation between the errors at $L = 16$ and $L = 24$.) We see that, within the 10% errors, the results at $L = 16$ and $L = 24$ are consistent. Thus possible $1/L$ terms are small; they are no larger than the errors, and could be considerably smaller. The $1/L$ terms should be smaller still at $\beta = 5.7$, for in physical units the lattices are larger.

Further evidence for the small size of $1/L$ terms comes from comparing the results to the predictions of chiral perturbation theory. In the chiral limit we expect $T_q = 1/4f_\pi^2$ and $T_g = 0$. Thus, for small quark masses, the infinite volume extrapolation of Q should yield $1/16f_\pi^2$. We include the results for this quantity in Table 5 and in Fig. 4. The chiral prediction works well for all three quark masses.

To illustrate this more clearly, we show in Fig. 5 the quantity $N_f Q f_\pi^2 = T_q f_\pi^2 + O(1/L)$ which should equal 1/4 in the simultaneous chiral and infinite volume limits. We have combined the errors in Q and f_π^2 in quadrature, ignoring correlations between these quantities. This plot allows us to include the data from $\beta = 5.7$. We plot the dimensionless amplitude against m_π^2 in physical units. It is striking that all the results are consistent with the chiral prediction, with no significant evidence for variation with m_π^2. Of course, as Table 5 and Fig. 4 show, Q itself does vary with m_π^2, but this is largely canceled by the variation in f_π^2.

We stress that we cannot extract a prediction for the mass dependence of the $I = 2$ amplitude $T_2 = T_q + T_g$, because we do not have results for T_g. This

is unfortunate, for it would allow an interesting comparison with the p^4 terms the chiral expansion [14]. What we can do is give a rough bound on the relative contribution of T_g, assuming that $T_g \approx G$. For $\beta = 6$ we use the results from the larger lattice. Remembering that $T_q \approx N_f Q$, we see from Table 5 that T_g is no larger than $\sim T_q/10$. Thus, although we cannot quantitatively check the prediction that T_g vanishes in the chiral limit, our results are qualitatively consistent with T_g being much smaller than T_q.

We can use Eqs. (7.3) to check that the $1/L$ corrections to T_q are expected to be as small as Fig. 4 implies. To do this, we assume $T_g = G$, and take the $t = 6 - 16$ values for G. Since G appears to be negative, and $c_1 = -2.84$ is also negative, T_q/N_f is predicted to be larger than Q. For $\beta = 5.7$ the increase is tiny: roughly 0.3(0.4)% for all masses, which is much smaller than the errors in Q. For $\beta = 6$, $L = 24$, the increase is larger, $3 - 6\%$, although still consistent with zero, and smaller than the errors in Q. Finally, for $\beta = 6$, $L = 16$, the increase is larger still, as large as 12%, although as discussed above, this should be considered to be an upper bound. Thus the maximum possible size of the shift is about the size of the error on Q. We conclude that the extraction of T_q is reliable.

If we undertake a similar exercise for T_g, however, we find that the $1/L$ term is comparable to or larger than the $O(1)$ term. Thus much larger volumes, in addition to reduced statistical errors, will be needed in order to extract T_g. This also underlines the approximate nature of the estimates of the $1/L$ terms in Q given in the previous paragraph.

Finally, we turn to the results involving non-Goldstone pion operators. We use these to check our understanding of the Fierz contributions to the Goldstone pion correlators. To do this we present a series of figures aimed at showing that Eq. (6.13) gives a reasonable representation of the data. We use the results with the smallest errors, which are those at $m_q = 0.03$ on the $L = 24$ lattices at $\beta = 6$. We begin by comparing the $\pi\pi \to \pi\pi$ and $\pi_3\pi_3 \to \pi_3\pi_3$ correlators. The crossed correlators are shown in Fig. 6a. If the scattering amplitudes for π and π_3 mesons are the same, as is true in the continuum limit, then the correlators should be the same. We find agreement at intermediate times where the π_3

correlator is not contaminated by boundary effects. This agreement indicates that staggered-flavor symmetry breaking is small.

The direct correlators are compared in Fig. 6b. Equation (6.13) predicts

$$\delta_D = D(t : \pi_3\pi_3 \to \pi_3\pi_3) - D(t : \pi\pi \to \pi\pi) = F(2t + H'(t) - 3H(t))Q/L^3 \ . \tag{7.4}$$

Since $H(t) = H'(t) + O(t^2) = t + O(t^2)$, the difference between the correlators should vanish at small t. This is also true in the limit that $\delta m_\pi \to 0$. As t increases, H' curves upwards, while H curves downwards, so that δ_D should be positive and increasing. The figure shows that these features are qualitatively correct. The solid line shows the prediction from Eq. (6.13) for the $\pi_3\pi_3 \to \pi_3\pi_3$ correlator, using the parameters obtained from the $t = 6 - 16$ fit to the $\pi\pi \to \pi\pi$ correlators. We stress that a global fit to all correlators would considerably improve the agreement, particularly if we allowed for some flavor symmetry breaking in the scattering, creation and annihilation amplitudes. The point we want to make is that the prediction is qualitatively correct, and in particular it matches the curvature of the data. The presence of this curvature is confirmation of the arguments leading to the functions $H(t)$ and $H'(t)$.

A more direct confirmation is provided by the crossed $\pi_3\pi_3 \to \pi\pi$ correlator. Eq. (6.13) predicts that

$$\delta_C = C(t : \pi_3\pi_3 \to \pi\pi) - C(t : \pi\pi \to \pi\pi) = Z(H(t) - t)Q/L^3 \ , \tag{7.5}$$

i.e. that the dominant linear term in the $\pi\pi \to \pi\pi$ correlator is replaced by the same term with $H(t)$ instead of t. Thus the curvature of $H(t)$ should be clear, and Fig. 7a confirms this expectation. The two correlators agree at small t and then diverge. The solid line gives the prediction of Eq. (6.13), which in this case works remarkably well.

The prediction for the direct $\pi_3\pi_3 \to \pi\pi$ correlator also works very well, as shown in Fig. 7b. Here what is being tested is that the signs from Fierz transforming and from the interaction vertex are correct. The prediction is that $D \propto (t - H(t))$, and the cancellation between t and $H(t)$ is evident from the figure.

Finally we show in Figs. 8 the results for the $\pi\pi \to \pi_3\pi_3$ correlators, together with our predictions. The dominant new feature of the crossed graph is the exponential decay in the Fierz term. This is well represented by our data, shown in Fig. 8a. The prediction does less well for the direct graph (Fig. 8b), although the general shape and magnitude is reasonably well reproduced.

8. Conclusions

We have shown that it is possible to do a reasonable job of extracting the $I = 2$ $\pi\pi$ scattering length from finite volume effects in lattice QCD. The dominant contribution to the amplitude, that due to "quark exchange", can be extracted reliably, while the subdominant "gluon exchange" amplitude cannot. The results are in good agreement with constraints of chiral symmetry. As a matter of principle this is not surprising, since in the staggered formalism one can derive Weinberg's and related formulae directly on the lattice. Still it is encouraging to find that with currently accessible statistics and parameter ranges, we can really claim to understand finite volume effects at the quantitative level.

Many of the technicalities encountered here are a result of the use of staggered fermions and of interpolating operators which create pions on the same timeslice. It would be interesting to simplify the analysis by repeating the calculation with separated pion sources, so that Fierz terms are absent. This could be done by using sources on different timeslices, or spatially separated sources on the same timeslice. Likewise it would be interesting to go through the same analysis with Wilson fermions, and such work is in progress [24].

Finally we note that in principle one could go ahead and calculate the $I = 0$ scattering length in the same way, even using the quenched approximation. Dynamical quark loops are essential to obtain the terms of $O(t^2)$ correctly, but one can use the term linear in t to extract the scattering amplitudes, as we have done here. Even so, the prospect is daunting, since such a calculation would involve calculating the statistically demanding single and double annihilation graphs.

Acknowledgements

We thank Claude Bernard, Julius Kuti, Heiri Leutwyler and Apoorva Patel for useful discussions. This study is made possible by a Grand Challenge Award at NERSC. We thank J. Mandula and T. Kitchens for their tremendous support. This work was partly supported by NSF Grant No. PHY89-04035 (supplemented by funds from NASA). SRS is also supported in part by DOE contract DE-AC05-84ER40150 and grant DE-FG06-91ER40614, and by an Alfred P. Sloan Fellowship.

Appendix A. Discussion of Lüscher's formula

Calculations of scattering amplitudes using staggered fermions face various difficulties. To overcome these it is useful to have a clear understanding of the source of the various terms in Lüscher's formula Eq. (2.2):

$$\delta E = \frac{T}{L^3}\left(1 - c_1\frac{m_\pi T}{4\pi L} + c_2\left(\frac{m_\pi T}{4\pi L}\right)^2\right) + O(L^{-6}) \ . \tag{A.1}$$

In this appendix we give a heuristic summary of Lüscher's analysis [1]. We use non-relativistic Quantum Mechanics (NRQM) to present the arguments, for Lüscher has shown how to take results from NRQM over to field theory.

Let the Hamiltonian H_0 describe non-relativistic non-interacting pions. We are interested in states containing two pions, which we label by their relative momentum:

$$H_0|\vec{p}\rangle = 2 \times \frac{\vec{p}^{\,2}}{2m}|\vec{p}\rangle = E_p|\vec{p}\rangle \ . \tag{A.2}$$

The states are normalized to unity in a box of length L. With periodic boundary conditions only momenta with $p_i = 2\pi n_i/L$ are allowed. We add a perturbing potential V, which depends only on the relative coordinate of the two pions, and has finite range. This shifts the energies of the states, and we are interested in this shift for the lightest two pion state, $|\vec{0}\rangle$. In perturbation theory this is

$$\begin{aligned}\delta E = \langle\vec{0}|V|\vec{0}\rangle &- \sum_{\vec{p}\neq 0}\frac{|\langle\vec{0}|V|\vec{p}\rangle|^2}{E_p} + \sum_{\substack{\vec{p}\neq 0\\ \vec{q}\neq 0}}\frac{\langle\vec{0}|V|\vec{p}\rangle\langle\vec{p}|V|\vec{q}\rangle\langle\vec{q}|V|\vec{0}\rangle}{E_p E_q} \\ &- \langle\vec{0}|V|\vec{0}\rangle\sum_{\vec{p}\neq 0}\frac{|\langle\vec{0}|V|\vec{p}\rangle|^2}{E_p^2} + O(V^4) \ .\end{aligned} \tag{A.3}$$

This is the NRQM equivalent of the δE we calculate in field theory.

Our aim is to use δE to extract the infinite volume scattering amplitude. The Born series for the non-relativistically normalized amplitude at threshold is

$$T = \langle\!\langle\vec{0}|V|\vec{0}\rangle\!\rangle - \int_p \frac{|\langle\!\langle\vec{0}|V|\vec{p}\rangle\!\rangle|^2}{E_p - i\epsilon} + \int_p\int_q \frac{\langle\!\langle\vec{0}|V|\vec{p}\rangle\!\rangle\langle\!\langle\vec{p}|V|\vec{q}\rangle\!\rangle\langle\!\langle\vec{q}|V|\vec{0}\rangle\!\rangle}{(E_p - i\epsilon)(E_q - i\epsilon)} + O(V^4) \ , \tag{A.4}$$

where $\int_p \equiv \int d^3p/(2\pi)^3$, and the states in this expression have continuum normalization $\langle\!\langle \vec{p}\,|\vec{q}\rangle\!\rangle = (2\pi)^3\delta(\vec{q}-\vec{p})$. For the amplitude at threshold, the integrals are infrared convergent and we can set $\epsilon = 0$. Thus T is real.

To compare T with δE we must account for the different normalizations, $\langle\!\langle \vec{p}\,|\vec{q}\rangle\!\rangle = L^3\langle\vec{p}\,|\vec{q}\rangle$. We also need to relate momentum sums and integrals. This is highly non-trivial because of the infrared singularities in the integrands, i.e. the factors of $1/E_p$. Were it not for these singularities, one would have the simple relation $\int_p = \sum_p /L^3$. It turns out that one can use this relation to determine the leading behavior in an expansion in powers of $1/L$ [1]. Doing so, we see that the first three terms in δE are equal to those in T/L^3, while the fourth term in δE is suppressed by a factor of $1/L^3$. This pattern remains true to all orders in the potential V: all terms in T/L^3 have corresponding terms in δE, while "extra" terms in δE are suppressed by powers of $1/L$. Thus, at leading order in $1/L$, the energy shift is related to the scattering amplitude by $\delta E = T/L^3$. The factor of $1/L^3$ can be understood physically. The two pions only interact when they overlap, for which the phase space is proportional to $1/L^3$.

To calculate the difference $\delta E - T/L^3$ we need to evaluate the difference between the sums in δE and integrals in T, and the "extra" terms in δE. We discuss these in turn.

1. *Momentum sums vs. integrals.* Consider the difference between the terms of $O(V^2)$ in δE and T/L^3. If $1/E_p = m/p^2$ were replaced by a smooth function whose derivatives were integrable at $\vec{p}=0$, then the difference would be zero (Eq. 2.42 of Ref. [1]). Thus the difference is dominated by the region around $\vec{p}=0$. A rough estimate is obtained from the part of the integral corresponding to the point excised from the sum, i.e. the point at $\vec{p}=0$. Naively, this gives a term in the difference of $O(1/L^6)$, but the infrared divergence in the integrand raises the power to $1/L^4$

$$\begin{aligned}\delta E - \frac{T}{L^3} &\approx -\frac{1}{L^3}\prod_{i=1}^{3}\left(\int_{-\pi/L}^{\pi/L} dp_i\right)\frac{|\langle\!\langle\vec{0}\,|V|\vec{p}\rangle\!\rangle|^2}{E_p} + O(V^3/L^4) \\ &\approx -\frac{8\pi^2 m}{L^3}\int_0^{\pi/L} p^2 dp \frac{|\langle\!\langle\vec{0}\,|V|\vec{0}\rangle\!\rangle|^2}{p^2} + O(V^3/L^4) \qquad \text{(A.5)} \\ &\propto \frac{1}{L^4}|\langle\!\langle\vec{0}\,|V|\vec{0}\rangle\!\rangle|^2 + O(V^3/L^4)\,,\end{aligned}$$

Lüscher's analysis gives the coefficient of proportionality to be $-c_1 m_\pi/4\pi$, with c_1 the known constant given in the text. This is the first term in the expansion of the T^2/L^4 term in Eq. (A.1) in powers of V.

At $O(V^3)$, we must consider the difference between the double sum in (A.3) and the double integral in (A.4). The contribution to this difference from the region where either $\vec{p}$ or $\vec{q}$ is close to zero is again of $O(1/L^4)$. It comes with the correct coefficient to contribute the $O(V^3)$ term in the T^2/L^4 term in Eq. (A.1). Lüscher shows this result to be true to all orders in V

$$\delta E - \frac{T}{L^3} = -c_1\frac{m_\pi T^2}{4\pi L^4} + O(\frac{1}{L^5})\,. \qquad \text{(A.6)}$$

It appears remarkable that the terms of different orders in V add up to give the series for T^2, but this can be understood on general grounds [2].

The difference between the $O(V^3)$ sum and integral also gives a term proportional to V^3/L^5, from the region in which both momenta are close to zero. This is one of the leading order contributions to the term proportional to T^3/L^5 in Eq. (A.1).

2. *"Extra" terms in δE.* The remainder of the V^3/L^5 terms come from the the fourth term in δE, which has no counterpart in T. Though naively of $O(1/L^6)$, the infra-red divergence $\sum 1/E_p^2$ raises the leading power to $1/L^5$. Lüscher shows that, to all orders in V, the $O(1/L^5)$ terms combine to give $c_2 T^3 m_\pi^2/(16\pi^2 L^5) + O(1/L^6)$.

It is helpful to extend this analysis to matrix elements of the Euclidean evolution operator, for these are the quantities we actually calculate. The analog of the ratio $R(t)$ in NRQM is

$$R(t) = \frac{\langle\vec{0}|e^{-(H_0+V)t}|\vec{0}\rangle}{\langle\vec{0}\,|e^{-H_0 t}|\vec{0}\rangle} = \langle\vec{0}|e^{-(H_0+V)t}|\vec{0}\rangle = Z_L e^{-\delta E t} + \ldots\,, \qquad \text{(A.7)}$$

where in the second equality we have used the fact that $E_0 = 0$. The ellipsis represents the contributions of higher states, and Z_L is the absolute square of the overlap between the true lightest state and $|\vec{0}\rangle$. In field theory Z_L becomes

the $Z_{\pi\pi}/Z_\pi^2$ of Eq. (2.6). Expanding the evolution operator in perturbation theory

$$e^{-(H_0+V)t} = e^{-H_0 t} - \int_0^t dt' e^{-H_0(t-t')} V e^{-H_0 t'} + \int_0^t dt' \int_0^{t'} dt'' e^{-H_0(t-t')} V e^{-H_0(t'-t'')} V e^{-H_0 t''} + \dots \ , \tag{A.8}$$

we have

$$R(t) = 1 - t\langle\vec{0}|V|\vec{0}\rangle + \int_0^t dt' \int_0^{t'} dt'' \sum_{\vec{p}} \langle\vec{0}|V|\vec{p}\rangle e^{-E_p(t'-t'')} \langle\vec{p}|V|\vec{0}\rangle + \dots \ . \tag{A.9}$$

Separating out the state with $\vec{p} = 0$ in the second term, and doing the integrals, gives

$$\begin{aligned} R(t) &= 1 - t\langle\vec{0}|V|\vec{0}\rangle + \tfrac{1}{2}t^2\langle\vec{0}|V|\vec{0}\rangle^2 + \sum_{\vec{p}\neq 0} \frac{|\langle\vec{0}|V|\vec{p}\rangle|^2}{E_p} \left(t + \frac{e^{-E_p t} - 1}{E_p} \right) + \dots \\ &= 1 - t\delta E_1 - t\delta E_2 + \tfrac{1}{2}(t\delta E_1)^2 + \sum_{\vec{p}\neq 0} \frac{(e^{-E_p t} - 1)|\langle\vec{0}|V|\vec{p}\rangle|^2}{E_p^2} + \dots \ . \end{aligned} \tag{A.10}$$

Here we are using the notation that δE_i is the contribution to δE of $O(V^i)$ (see Eq. (A.3)).

We can interpret this result in the following way. As the expansion Eq. (A.8) shows, the two pions propagate freely except for interactions due to V. The factor of 1 on the right hand side of Eq. (A.10) corresponds to the pions propagating without interaction. The $-t\delta E_1$ term corresponds to a single interaction; there is a factor of t since the interaction can happen at any intermediate time.[7] If there are two interactions, the interpretation depends on whether the intermediate state is "on-shell" (i.e. $|\vec{0}\rangle$) or "off-shell". In the former case, the pions are propagating freely except for two interactions, which leads to the factor $\frac{1}{2}t^2$ multiplying δE_1^2. This clearly extends to higher orders; n scatterings

[7] The minus sign is an artifact of the non-relativistic definition of T. Using T_R the sign is positive, as expected intuitively.

with all intermediate states being on-shell leads to $(-\delta E_1 t)^n/n!$, which builds up an exponential series.

We now return to the $O(V^2)$ terms with off-shell intermediate states. These give rise to $-t\delta E_2$ in the following way. Since the intermediate states are off-shell, the two interactions are close in time, and can be thought of as a single interaction, of finite time extent, and of strength δE_2. This composite interaction can occur at any time, leading to the factor of t. The same picture applies for terms of higher order in V in which all intermediate states are off-shell. These add up to a composite interaction of strength $\delta E + O(1/L^5)$, the $1/L^5$ deviation appearing because the "extra" terms in δE are not produced. Thus the term linear in t is $-t(\delta E + O(1/L^5))$. Since $\delta E = T/L^3 + O(1/L^4)$, we can think of the t term as coming from two pions propagating freely except for a single all-orders scattering which can occur at any time, the $1/L^3$ being the overlap factor.

Similarly, higher order terms convert $\delta E_1^2 t^2/2$ into $\delta E^2 t^2/2$ plus corrections suppressed by powers of $1/L$. This can be thought of as due to two all-orders scatterings. The t and t^2 terms are themselves building up the exponential $\exp(-\delta E t)$ which is the dominant part of R at large times.

The corrections to this interpretation come from edge effects. For example, the off-shell $O(V^2)$ term does not give precisely $-t\delta E_2$, because the finite time extent of the interaction is not properly accounted for at the beginning and ending times. The difference is the last term in Eq. (A.10). This has two components: a term falling exponentially and a constant. The former comes from mixing with more energetic eigenstates of $H_0 + V$ and is unimportant at large times. The latter gives the first term in the difference between $\exp -t\delta E$ and the correct expression $Z_L \exp -t\delta E$ (Eq. (A.7)). Z_L differs slightly from unity, and indeed the constant part of the final term in Eq. (A.10) is the standard NRQM expression for $Z_L - 1$. It is important to note that, although $Z_L - 1$ is naively of $O(1/L^3)$, the infrared divergence alters the behavior to $O(1/L^2)$. This is true to all orders in V. Thus, if one were to ignore wavefunction renormalization, and use the coefficient of term linear in t in Eq. (A.10) to determine δE, one would be making an fractional error of $O(1/L^2)$. But since $\delta E \propto 1/L^3$, this

corresponds to an absolute error proportional to $1/L^5$. We use this result in the text.

Higher orders in V give rise to further terms in $\exp(-t\delta E)$, and to higher order wave function renormalizations. For the discussion of staggered-flavor symmetry breaking in section 5, we need to know the effect of contributions in which one or more of the intermediate states is on-shell. It is straightforward to see that these contribute to (i) terms quadratic or higher order in t; (ii) terms linear in t which are part of $(1 - Z_L)\delta E t$, and thus proportional to t/L^5; and (iii) constant terms in $(1 - Z_L)$ which are thus of $O(1/L^2)$.

Appendix B. Staggered fermion Ward identities

In this appendix we use lattice chiral Ward identities to derive expressions for the amplitudes T_q and T_g (Eq. (4.4)) close to the chiral limit. These results agree with Weinberg's continuum predictions, which we discuss in section 4. We also can make predictions for the form in configuration space of a two pion correlator similar to that we actually study.

We begin with T_q, which is defined to be the scattering amplitude obtained from the average of the crossed diagram of Fig. 1b with the diagram in which the arrows are reversed. This averaging is equivalent to taking the real part of Fig. 1b alone. Our discussion uses the notation and methods of Ref. [11]. We work in infinite volume, with $n_i = (\vec{n}_i, \tau_i)$ labeling the Euclidean position of the i'th pion, and assume that we are close to the continuum limit so that we can approximate $2\sin(p_\mu/2)$ by p_μ, etc. Using translation invariance to fix $n_4 = (\vec{0}, 0)$, the crossed diagram correlator is

$$C_{4\pi}(n_1, n_2, n_3) = -(-1)^{n_1+n_2+n_3}\langle \mathrm{Re}\,[\overline{\chi}_a\chi_b(n_1)\overline{\chi}_c\chi_d(n_2)\overline{\chi}_b\chi_c(n_3)\overline{\chi}_d\chi_a(0)]\rangle \ , \tag{B.1}$$

where the expectation value indicates the full functional integral over gluon and quark fields. The sole purpose of the fake flavor indices $a - d$ is to restrict the Wick contractions to those of Fig. 1b. The pion interpolating field is chosen to be local since this form is convenient to derive Ward identities. The minus sign

in Eq. (B.1) is designed to cancel the sign from Fermi statistics so that upon integrating out the fermions we have

$$C_{4\pi}(n_1, n_2, n_3) = (-1)^{n_1+n_2+n_3}\langle \mathrm{Re}\,\mathrm{Tr}\,[G(0; n_1)G(n_1; n_3)G(n_3; n_2)G(n_2; 0)]\rangle \ , \tag{B.2}$$

which is similar to, and has the same sign as, the correlator C_{stagg} that we actually calculate. The expectation value now indicates an integral over only gauge fields, with G the quark propagator in this background field.

Various symmetries of $C_{4\pi}$ will be important in the following. These are symmetry under (i) $(1 \leftrightarrow 2)$ exchange: $C_{4\pi}(n_1, n_2, n_3) = C_{4\pi}(n_2, n_1, n_3)$; (ii) $(3 \leftrightarrow 4)$ exchange; and (iii) $(12 \leftrightarrow 34)$ exchange. These can be seen using $G(n_i; n_j)^\dagger = (-1)^{n_i+n_j}G(n_j; n_i)$.

We wish to extract the scattering amplitude from the correlator. To do this it is convenient to work in momentum space

$$C_{4\pi}(p_1, p_2, p_3) = \sum_{n_1,n_2,n_3} \exp[i(p_1\cdot n_1 + p_2\cdot n_2 + p_3\cdot n_3)]\, C_{4\pi}(n_1, n_2, n_3) \ . \tag{B.3}$$

Here p_i is the momentum flowing into the i'th pion, and $p_4 = -(p_1 + p_2 + p_3)$. To extract the amplitude we must analytically continue to the poles at $p_i^2 = m_\pi^2$. First we must define the renormalization constant Z_π:

$$C_\pi(p_1) = \sum_{n_1} \exp(ip_1\cdot n_1)C_\pi(n_1) = \frac{Z_\pi}{p_1^2 + m_\pi^2} + \mathrm{regular} \ , \tag{B.4}$$

where

$$C_\pi(n_1) = (-1)^{n_1}\langle \mathrm{Tr}\,[G(0; n_1)G(n_1; 0)]\rangle \ . \tag{B.5}$$

Using this we write

$$C_{4\pi}(p_1, p_2, p_3) = \prod_i^4 \left(\frac{\sqrt{Z_\pi}}{p_i^2 + m_\pi^2}\right) \mathcal{A}_{4\pi} \ , \tag{B.6}$$

for then, using the reduction theorem, $\mathcal{A}_{4\pi}$ is the scattering amplitude when we go on-shell. In fact, because of the sign in the definition (B.1), and because of the staggered fermion flavor factor discussed in section 5, this amplitude must be multiplied by $-N_f$ to be compared with the continuum scattering amplitude.

We can go on-shell in three ways, and thus obtain from $\mathcal{A}_{4\pi}$ the $1+2 \to 3+4$ (s-channel), $1+3 \to 2+4$ (t-channel), and $1+4 \to 2+3$ (u-channel) scattering amplitudes. In the s-channel the scattering takes place by quark exchange, but for t- and u-channels the scattering is by single-annihilation. We now make the crucial assumption, namely that $\mathcal{A}_{4\pi}$ depends smoothly on the momenta and the squared pion mass, so that we can write

$$\mathcal{A}_{4\pi} = \alpha + \beta m_\pi^2 + \gamma(p_1^2+p_2^2+p_3^2+p_4^2) + \tfrac{1}{2}\delta[(p_1+p_2)^2+(p_3+p_4)^2] + \ldots , \quad \text{(B.7)}$$

where α, β, γ and δ are constants. The ellipsis represent terms higher order in momenta and masses, including the non-analytic terms arising from pion loops, which we ignore. Invariance under discrete lattice rotations ensures the absence of terms linear in p_i and that the $O(p^2)$ terms appear as four-vector inner products. The symmetries under $(1 \leftrightarrow 2)$, $(3 \leftrightarrow 4)$ and $(12 \leftrightarrow 34)$ exchanges also restrict the $O(p^2)$ terms. In sum, through $O(p^2)$ we end up with the same expression one would find in the continuum.

If we can determine the constants in Eq. (B.7), then we can find a relationship between the three physical scattering amplitudes which are contained in $\mathcal{A}_{4\pi}$. We return to the precise form of this relationship below.

To fix the constants we begin with a lattice version of Adler's theorem. For $p_3 = 0$, with the other particles on-shell,[8] the relevant Ward identity is

$$\sum_{n_3} C_{4\pi}(n_1, n_2, n_3) = \frac{1}{2m_q}\left(C_{\pi\epsilon\pi}(n_1, n_2) + C_{\pi\epsilon\pi}(n_2, n_1)\right) , \quad \text{(B.8)}$$

which relates the pion four-point function to a pion-pion-scalar three point function

$$C_{\pi\epsilon\pi}(n_1, n_2) = (-1)^{n_1}\langle \mathrm{Re}\,\mathrm{Tr}\,[G(0;n_1)G(n_1;n_2)G(n_2;0)]\rangle . \quad \text{(B.9)}$$

In momentum space this corresponds to

$$C_{4\pi}(p_1, p_2, p_3=0) = \frac{1}{2m_q}\left(C_{\pi\epsilon\pi}(p_1, p_2) + C_{\pi\epsilon\pi}(p_2, p_1)\right) . \quad \text{(B.10)}$$

[8] This is possible with imaginary momenta, e.g. (with $i=\sqrt{-1}$) $p_1 = \frac{1}{2}im_\pi(1, \sqrt{3}, 0, 0)$, $p_2 = \frac{1}{2}im_\pi(1, -\sqrt{3}, 0, 0)$, $p_4 = -p_1 - p_2$.

The absence of the factor $(-1)^{n_2}$ in Eq. (B.9) implies that the interpolating operator at n_2 is a scalar, so that $C_{\pi\epsilon\pi}(p_1, p_2)$ does not have a pole at $p_2^2 = -m_\pi^2$. Thus both terms on the right hand side of Eq. (B.10) are lacking one of the poles of the left hand side. Multiplying by $(p_1^2+m_\pi^2)(p_2^2+m_\pi^2)(p_4^2+m_\pi^2)$ and going to the poles, yields

$$\mathcal{A}_{4\pi}(p_1^2=p_2^2=p_4^2=-m_\pi^2; p_3=0) = 0 . \quad \text{(B.11)}$$

Inserting the parameterization (B.7) into this result, and noting that $(p_1+p_2)^2 = -m_\pi^2$, gives the condition

$$\alpha + (\beta - 3\gamma - \delta)m_\pi^2 = 0 . \quad \text{(B.12)}$$

This must hold for all (sufficiently small) values of m_π^2, so we deduce that

$$\alpha = 0 \qquad \text{and} \quad \beta = 3\gamma + \delta . \quad \text{(B.13)}$$

The same result follows from setting any of the other momenta to zero.

The second constraint comes from setting $p_1 = p_2 = 0$. The Ward identity is

$$\sum_{n_1,n_2} C_{4\pi}(n_1, n_2, n_3) = \frac{1}{2m_q^2}\left(C_\pi(n_3) + C_\epsilon(n_3)\right) , \quad \text{(B.14)}$$

where the pion correlator is defined in Eq. (B.5), and the scalar correlator is

$$C_\epsilon(n_3) = \langle \mathrm{Tr}\,[G(0;n_3)G(n_3;0)]\rangle . \quad \text{(B.15)}$$

Fourier transforming Eq. (B.14), and comparing the coefficients of the poles at $p_3^2 = p_4^2 = -m_\pi^2$, to which the scalar correlator does not contribute, we find

$$\frac{Z_\pi^2}{m_\pi^4(p_3^2+m_\pi^2)^2}(\alpha + \beta m_\pi^2 + 2\gamma p_3^2 + O(p^4)) = \frac{Z_\pi}{2m_q^2(p_3^2+m_\pi^2)}(1 + O(p_3^2+m_\pi^2)) . \quad \text{(B.16)}$$

To cancel the double pole on the left hand side requires

$$\alpha = 0 \qquad \text{and} \quad \beta = 2\gamma , \quad \text{(B.17)}$$

while to match the coefficient of the single pole we must have

$$\beta = \frac{m_\pi^4}{2m_q^2 Z_\pi} = \frac{1}{N_f f_\pi^2} \ . \tag{B.18}$$

The second equality in this equation follows from the result [11]

$$\sqrt{\frac{Z_\pi}{2N_f}} = \frac{f_\pi m_\pi^2}{2m_q} \ . \tag{B.19}$$

Combining Eqs. (B.13) and (B.17) we obtain the final relation

$$\delta = -\gamma = -\frac{\beta}{2} \ . \tag{B.20}$$

An interesting check on these results is obtained by setting $p_1 = p_3 = 0$, so that

$$\mathcal{A}_{4\pi} = \alpha + \beta m_\pi^2 + (2\gamma + \delta)p_2^2 = \frac{m_\pi^4}{2m_q^2 Z_\pi}\left(m_\pi^2 + \frac{p_2^2}{2}\right) \ . \tag{B.21}$$

In momentum space the Ward identity is

$$C_{4\pi}(0, p_2, 0) = \frac{1}{4m_q^2}\left(C_\pi(p_2) + C_\epsilon(p_2) + \frac{dC_\pi(p_2)}{dm}\right) \ . \tag{B.22}$$

As before, the left hand side has a double pole, but here it is not canceled by the numerator of Eq. (B.21). Instead, the right hand side has a double pole from the derivative of the pion propagator. Inserting the relations (B.17) and (B.20) one finds that the coefficients of single and double poles match.

Using the results for the coefficients, we can rewrite the amplitude as

$$\mathcal{A}_{4\pi} = \frac{2m_\pi^2 - t - u}{2N_f f_\pi^2} + O(m_\pi^2 \ln(m_\pi^2)) \ , \tag{B.23}$$

where, as usual, $t = -(p_1 + p_3)^2$ and $u = -(p_1 + p_4)^2$. From this we can extract the scattering length and effective range for both the quark-exchange and annihilation amplitudes. To do this we must multiply by the factor $-N_f$ as noted above. The relativistically normalized quark-exchange amplitude at threshold is then

$$T_q^R = -N_f \mathcal{A}_{4\pi}(t = u = 0) = -\frac{m_\pi^2}{f_\pi^2} + O(m_\pi^2 \ln(m_\pi^2)) \ . \tag{B.24}$$

In fact, since the direct diagram vanishes at leading order in m_π^2, as discussed below, this is also the result for $T(\mathbf{S})^R$. To convert this to the non-relativistically normalized amplitude T_q, we use

$$T_q = \frac{-T_q^R}{4m_\pi^2} = \frac{1}{4f_\pi^2} + O(m_\pi^2 \ln(m_\pi^2)) \ . \tag{B.25}$$

This is the main result of the appendix. The important point is that it agrees with the Weinberg's continuum result. The derivation does not depend on the lattice spacing, nor on whether the quenched approximation is used.

It is instructive to compare the lattice off-shell amplitude with that from the chiral Lagrangian. Using a four-flavor Lagrangian (Eq. (4.2)), choosing pion flavors appropriately (Eq. (3.3)), and dividing by $-N_f$, we find

$$-\frac{\mathcal{A}_{4\pi}^{\rm cont}}{N_f} = -\frac{1}{N_f f_\pi^2}\left(\frac{t+u}{2} + \frac{m_\pi^2 + p_1^2 + p_2^2 + p_3^2 + p_4^2}{3}\right) + O(m_\pi^2 \ln(m_\pi^2)) \ . \tag{B.26}$$

This differs from the lattice result Eq. (B.23): the $t + u$ terms agree, but the m_π^2 terms do not. If we go on-shell, however, i.e. $p_i^2 = -m_\pi^2$, then the two results agree. The off-shell amplitudes can disagree because the two methods use different interpolating fields for the pions.

We note in passing that we can extract the single-annihilation amplitude at threshold (Fig. 1c) from Eq. (B.23):

$$T_{\rm ann}^R = -N_f \mathcal{A}_{4\pi}(t = 4m_\pi^2, u = 0) = \frac{m_\pi^2}{f_\pi^2} + O(m_\pi^2 \ln(m_\pi^2)) \ , \tag{B.27}$$

i.e. $T_{\rm ann}^R = -T_q^R$ at leading order.

Having determined the correlator to leading order in m_π^2 we can study it in configuration space. This is interesting because we can construct a correlator similar to the quantity $C(\tau)$ which we actually calculate. There is a small slight of hand involved, however, since the results derived above were in infinite volume. We simply assume that Eqs. (B.6) and (B.23) are valid in large volumes. To construct our look-alike of $C(\tau)$ we first Fourier transform back to Euclidean time, keeping the spatial momenta equal to zero

$$C_{4\pi}(\tau_1, \tau_2, \tau_3) \equiv \sum_{\vec{n}_1, \vec{n}_2, \vec{n}_3} C_{4\pi}((\vec{n}_1, \tau_1), (\vec{n}_2, \tau_2), (\vec{n}_3, \tau_3)) \ . \tag{B.28}$$

We next place the first two pions on one timeslice, $\tau_1 = \tau_2 = \tau$, and put the third on the same timeslice as the fourth, $\tau_3 = 0$. A straightforward calculation using Eqs. (B.6) and (B.23) yields, for $\tau >> 0$

$$N_f C_{4\pi}(\tau,\tau,0) = \frac{Z_\pi^2}{16 f_\pi^2 m_\pi^2} \tau e^{-2m_\pi \tau} \tag{B.29}$$

The correlator in Eq. (B.29) differs from that we actually calculate (Eq. (2.3)) in two respects. First, we use wall sources rather than point sources at $\tau = 0$. This should be unimportant if we take the ratio of $C_{4\pi}$ to the product of the appropriate two pion propagators, in which the source amplitudes cancel. Overlap terms, which will be source dependent, are suppressed by $1/L^2$, as discussed in appendix A. Thus at large τ we expect the correlator $C(\tau)$ which we calculate to be well described by

$$\frac{N_f C_{4\pi}(\tau,\tau,0)}{L^3 C_\pi(\tau)^2} = \frac{\tau}{4 f_\pi^2 L^3} = \frac{\tau T_g}{L^3} \ . \tag{B.30}$$

Here $C_\pi(\tau) = \sum_{\vec{n}} C_\pi(\tau,\vec{n})$ (see Eq. (B.5)), and the factor of L^3 arises because $\vec{n}_3$ is summed over.

Eq. (B.30) is exactly the form we expect for $C(\tau)$ if we keep only terms of $O(1/L^3)$ (see Eq. (6.6)). The absence of wave function renormalization terms (e.g. constants of $O(1/L^2)$) is due to our approximate treatment of finite volume effects.

For very large τ the correlator $C(\tau)$ must fall exponentially, which appears to contradict the result (B.30). There is no inconsistency, however, because the terms of quadratic and higher order in τ which build up the exponential result from multiple scattering. They are thus suppressed by powers of m_π^2, and are not included in our analysis. To see them we would have to do an honest finite volume calculation.

Finally, we discuss the Ward identities for the gluon exchange diagram and their consequences for T_g. The notation is simplified if we consider the double-annihilation diagram Fig. 1d, for then the symmetries are the same as for the crossed diagram considered above. We can obtain the gluon exchange

amplitude of Fig. 1a by a suitable choice of momenta. In place of Eq. (B.2) we have

$$C'_{4\pi}(n_1,n_2,n_3) = (-1)^{n_1+n_2+n_3}\langle \mathrm{Tr}\,[G(n_1;n_2)G(n_2;n_1)]\,\mathrm{Tr}\,[G(n_3;0)G(0;n_3)]\rangle \ . \tag{B.31}$$

We follow the same steps that lead from Eqs. (B.2) to (B.7), with Eqs. (B.8) and (B.9) replaced by

$$\sum_{n_3} C'_{4\pi}(n_1,n_2,n_3) = \frac{1}{m_q}(-1)^{n_1+n_2}\langle \mathrm{Tr}\,[G(n_2;n_1)G(n_1;n_2)]\,(\mathrm{Tr}[G(0;0)] - \langle \mathrm{Tr}[G(0;0)]\rangle)\rangle \ . \tag{B.32}$$

Since the operator at the origin is a scalar, there is no pole at $p_4^2 = -m_\pi^2$. This has two consequences. First, just as before this implies the relations (B.13). Second, using these relations in (B.5) and (B.7) gives

$$C'_{4\pi}(p_1,p_2,p_3{=}0) = \frac{Z_\pi^2}{m_\pi^2}\Big(\frac{\gamma}{(p_1^2+m_\pi^2)(p_4^2+m_\pi^2)} + \frac{\gamma}{(p_2^2+m_\pi^2)(p_4^2+m_\pi^2)} + \frac{\gamma+\delta}{(p_1^2+m_\pi^2)(p_2^2+m_\pi^2)}\Big) \ , \tag{B.33}$$

so that $\gamma = 0$ is required to remove the pole in p_4.

Next we set $p_1 = 0$ so that $p_2 = -p_4$, we find

$$C'_{4\pi}(p_1{=}0,p_2,p_3{=}0) = \frac{Z_\pi^2}{m_\pi^4}\frac{\delta}{(p_2^2+m_\pi^2)} = \frac{1}{m_q^2}\sum_{n_2}\exp(ip_2\cdot n_2)\langle \mathrm{Tr}[G(n_2;n_2)]\,(\mathrm{Tr}[G(0;0)] - \langle \mathrm{Tr}[G(0;0)]\rangle)\rangle \ . \tag{B.34}$$

The term on the right hand side does not have a pole at $p_2 = -m_\pi^2$, since the operator is a scalar, which implies that $\delta = 0$.

In summary, we find $\alpha = \beta = \gamma = \delta = 0$, so that that the double-annihilation amplitude and the gluon exchange amplitude vanish at $O(p^2, M)$. This implies that

$$T_g = O(m_\pi^2 \ln(m_\pi^2)) \ , \tag{B.35}$$

in agreement with the results from the chiral Lagrangian.

Appendix C. Transfer matrix interpretation of $R_2(t)$

To calculate the scattering amplitude T_2, or more generally to calculate the amplitude for the **S** representation in an $SU(N \geq 4)$ flavor theory, we use the quantity $R_2(t) = D_{\rm stagg}(t) - N_f C_{\rm stagg}(t)$ (Eqs. (3.1) and (5.1)). As explained in section 5, the diagrams that contribute to R_2 become, in the continuum limit, the same diagrams as those in the calculation of T_2 in QCD, or $T(\mathbf{S})$ in an $SU(N)$ theory. Thus, in the continuum limit, the exponential fall-off of $R_2(t)$ at large times gives δE, from which (using Eq. (2.2)) one can extract T. While this diagrammatic argument is reasonable, it is not a proof, for the diagrams that one draws for QCD are purely formal objects. This appendix aims to bolster the diagrammatic argument by showing how, for the particular case of a theory with $SU(4N_f)$ symmetry, one can indeed extract $T(\mathbf{S})$ from the exponential fall-off of $R_2(t)$. We are restricted to $4N_f$ flavors because this is the number required to define correlators which pick out $D_{\rm stagg}$ and $C_{\rm stagg}$, and to have a well defined transfer matrix we must also have $4N_f$ dynamical quarks.

First consider the direct diagram, Fig 1a. $D(t)$ can be obtained from the correlator $\langle \mathcal{O}_a \mathcal{O}_a^\dagger \rangle$ of the operator

$$\mathcal{O}_a = \mathrm{Tr}(\overline{U}\gamma_5 D T_5)\,\mathrm{Tr}(\overline{S}\gamma_5 C T_5)\ . \tag{C.1}$$

Only the flavor dependence is shown, the position dependence being as in Eq. (2.3).

To determine which scattering amplitude we can extract from $\langle \mathcal{O}_a \mathcal{O}_a^\dagger \rangle$, we need to know which representations of $SU(4N_f)$ are contained in the symmetric two pion state. As discussed in Section 3, the decomposition is into a singlet, an adjoint, and the **S** and **A** representations. We wish to calculate $T(\mathbf{S})$, the scattering amplitude for the **S** representation. To exhibit the flavor content of $\mathcal{O}_a$, it is useful to show the four staggered flavors explicitly. Labeling these 1-4, choosing a diagonal γ_5, and adopting the notation $\overline{u}_i \gamma_5 d_i \equiv (u_i d_i)$, we have

$$\mathcal{O}_a = (u_1 d_1 + u_2 d_2 - u_3 d_3 - u_4 d_4)\,(s_1 c_1 + s_2 c_2 - s_3 c_3 - s_4 c_4)\ . \tag{C.2}$$

Each of the sixteen terms in this product couples to an **S**+**A** combination. For example

$$(u_1 d_1)(s_1 c_1) = \frac{(u_1 d_1)(s_1 c_1) + (s_1 d_1)(u_1 c_1)}{2} + \frac{(u_1 d_1)(s_1 c_1) - (s_1 d_1)(u_1 c_1)}{2}\ . \tag{C.3}$$

The first term on the right hand side is part of an **S** representation since it is symmetric under quark exchange and all four flavors are different. Similarly, the second term is contained in an **A**.

Now, as discussed in section 4, the pion interaction is attractive in the **A** representation, but repulsive in the **S**, as long as one is close to the chiral limit. Thus the **A** components will dominate at large Euclidean time, so that the $\langle \mathcal{O}_a \mathcal{O}_a^\dagger \rangle$ alone is not useful for the purpose of studying T(**S**).

For this we add in the crossed diagram, Fig. 1b. We can obtain $-N_f C_{\rm stagg}$ from the correlator $\langle \mathcal{O}_a \mathcal{O}_b^\dagger \rangle$, in which

$$\begin{aligned} \mathcal{O}_b &= N_f\,\mathrm{Tr}(\overline{S}\gamma_5 D T_5)\,\mathrm{Tr}(\overline{U}\gamma_5 C T_5) \\ &= N_f (s_1 d_1 + s_2 d_2 - s_3 d_3 - s_4 d_4)\,(u_1 c_1 + u_2 c_2 - u_3 c_3 - u_4 c_4)\ . \end{aligned} \tag{C.4}$$

$\mathcal{O}_b$ also couples to sixteen **S** and sixteen **A** representations. Many of these representations do not, however, appear in $\mathcal{O}_a$ (Eq. (C.2)). The four representations in common are those in which the quarks and antiquarks all have the same staggered-flavor index. Expressing these in terms of **S** and **A** we have, for example

$$(s_1 d_1)(u_1 c_1) = \frac{(u_1 d_1)(s_1 c_1) + (s_1 d_1)(u_1 c_1)}{2} - \frac{(u_1 d_1)(s_1 c_1) - (s_1 d_1)(u_1 c_1)}{2}\ . \tag{C.5}$$

Thus $\langle \mathcal{O}_a \mathcal{O}_b^\dagger \rangle$ is also dominated by the **A** components at long times, but, compared to $\langle \mathcal{O}_a \mathcal{O}_a^\dagger \rangle$, they come in with opposite sign. Furthermore, although there are only 4 propagating components, compared to 16 in $\langle \mathcal{O}_a \mathcal{O}_a^\dagger \rangle$, each is multiplied by the overall factor of N_f. Thus the total **A** contribution to $\langle \mathcal{O}_a \mathcal{O}_b^\dagger \rangle$ is exactly opposite to that in $\langle \mathcal{O}_a \mathcal{O}_a^\dagger \rangle$. This means that the **A** component cancels in the sum of the two correlators, leaving the **S** component we wish to find. If we wish, we can also pick out the **A** component by taking the difference of $\langle \mathcal{O}_a \mathcal{O}_a^\dagger \rangle - \langle \mathcal{O}_a \mathcal{O}_b^\dagger \rangle$ (corresponding to $D + N_f C_{\rm stagg}$). Clearly, the factor of N_f in Eq. (5.1) is necessary to obtain these cancellations.

References

[1] M. Lüscher, *Commun. Math. Phys.* **104** (1986) 177; **105** (1986) 153

[2] M. Lüscher, *Nucl. Phys.* **B354** (1991) 531

[3] B.S. DeWitt, *Phys. Rev.***103** 1565 (1956)

[4] H.W. Hamber, E. Marinari, G. Parisi and C. Rebbi, *Nucl. Phys.* **B225** (1983) 475

[5] L. Maiani and M. Testa, *Phys. Lett.* **245B** (1990) 585

[6] C. Michael, *Nucl. Phys.* **B327** (1989) 515

[7] U. Wiese, in *"Lattice '88"*, proceedings of the 1988 Symposium on Lattice Field Theory, Batavia, Illinois, 1988, edited by A.S. Kronfeld and P.B. Mackenzie, *Nucl. Phys.* **B** (*Proc. Suppl.*) **9** (1989) 609

[8] T. DeGrand, *Phys. Rev.* **D43** (1991) 2296

[9] M. Lüscher, *Nucl. Phys.* **B364** (1991) 237

[10] S. Weinberg, *Phys. Rev. Lett.* **17** (1966) 616

[11] G.W. Kilcup and S.R. Sharpe, *Nucl. Phys.* **B283** (1987) 493

[12] M. Guagnelli, E. Marinari and G. Parisi, *Phys. Lett.* **240B** (1990) 188

[13] S. Sharpe, in in *"Lattice '90"*, proceedings of the International Conference on Lattice Field Theory, Tallahassee, Florida, 1990, edited by U.M. Heller, A.D. Kennedy, and S. Sanielevici, *Nucl. Phys.* **B** (*Proc. Suppl.*) **20** (1991) 406

[14] J. Gasser and H. Leutwyler, *Phys. Lett.* **125B** (1983) 325

[15] J. Gasser and H. Leutwyler, *Ann. Phys. (N.Y.)* **158** (1984) 142

[16] N. Kawamoto and J. Smit, *Nucl. Phys.* **B192** (1981) 100

[17] S. Sharpe, in *"Hadronic Matrix Elements and Weak Decays"*, proceedings of the Ringberg Workshop, Ringberg Castle, Germany, 1988, edited by A.J. Buras, J.-M. Gérard, and W. Huber *Nucl. Phys.* **B** (*Proc. Suppl.*) **7A**(1989) 255 .

[18] C. Bernard and A. Soni, in *"Lattice '88"*, proceedings of the 1988 Symposium on Lattice Field Theory, Batavia, Illinois, 1988, edited by A.S. Kronfeld and P.B. Mackenzie, *Nucl. Phys.* **B** (*Proc. Suppl.*) **9** (1989) 155

[19] H. Kluberg-Stern, A. Morel, O. Napoly and B. Petersson, *Nucl. Phys.* **B251** (1985) 581

[20] For a discussion of the dependence of the corrections on a see S. Sharpe, talk at "Lattice 91", Tsukuba, Japan, November 1991, to appear in the proceedings, CEBAF preprint CEBAF-TH-92-01

[21] M.F.L. Golterman, *Nucl. Phys.* **B273** (1986) 663

[22] R. Gupta, G. Guralnik, G. Kilcup and S. Sharpe, *Phys. Rev.* **D43** (1991) 2003

[23] R. Gupta, G. Guralnik, G. Kilcup, A. Patel, S. Sharpe and T. Warnock, *Phys. Rev.* **D36** (1987) 2183

[24] D. Daniel, R. Gupta, G. Kilcup, A. Patel and S. Sharpe, in progress

Figure Captions

Fig. 1: Diagrams contributing to two pion correlation functions: (a) "direct" or "gluon exchange"; (b) "crossed" or "quark exchange"; (c) "single annihilation": and (d) "double annihilation". The lines represent quark and anti-quark propagators in a background gluon field.

Fig. 2: The $\pi\pi \to \pi\pi$ crossed correlator $C_{staggs}(t) = C(t)/N_f$, on the three sets of lattices: (a) $\beta = 5.7$, $16^3 \times 32$; (b) $\beta = 6$, $16^3 \times 40$ (with some points at $m_q = 0.02$ removed for clarity); (c) $\beta = 6$, $24^3 \times 40$. The lines show the fits to the expected form, Eq. 6.13. The solid part of the line shows the region to which fitting was actually done, $t = 6 - 16$.

Fig. 3: The $\pi\pi \to \pi\pi$ direct correlator $D(t)$, with notation as in Fig. 2. For clarity, points from the lightest two masses are vertically offset. The offset values of unity are indicated by the short horizontal lines. The lines show the fitted function (Eq. 6.13), including the curvature caused by $H(t)$, even though the fit is actually made to the linear approximation to this function in the fit range. In (c) some of the errors are excluded for clarity.

Fig 4: Volume dependence of Q at $\beta = 6$. The values at $m_\pi/L \approx 0$ (some offset horizontally for clarity) are the intercepts expected in the chiral limit: $Q(L = \infty) = 1/(16 f_\pi^2)$.

Fig. 5: Testing the chiral prediction for the scattering amplitude. Results for $N_f Q f_\pi^2 = T_q f_\pi^2 + O(1/L)$. The expected chiral limit is $1/4$.

Fig. 6: Comparing $\pi_3\pi_3 \to \pi_3\pi_3$ to $\pi\pi \to \pi\pi$ correlators at $\beta = 6$, $L = 24$, $m_q = 0.03$: (a) $C_{staggs}(t)$; (b) $D(t)$, with the solid line showing the expected result (not a fit) for the $\pi_3\pi_3 \to \pi_3\pi_3$ correlator using Eq. 6.13.

Fig 7: The $\pi_3\pi_3 \to \pi\pi$ correlators at $\beta = 6$, $L = 24$, $m_q = 0.03$, together with predictions from Eq. 6.13: (a) $C_{staggs}(t)$, compared to the $\pi\pi \to \pi\pi$ correlator; (b) $D(t)$.

Fig. 8: The $\pi\pi \to \pi_3\pi_3$ correlators at $\beta = 6$, $L = 24$, $m_q = 0.03$, together with predictions from Eq. 6.13: (a) $C_{staggs}(t)$; (b) $D(t)$.

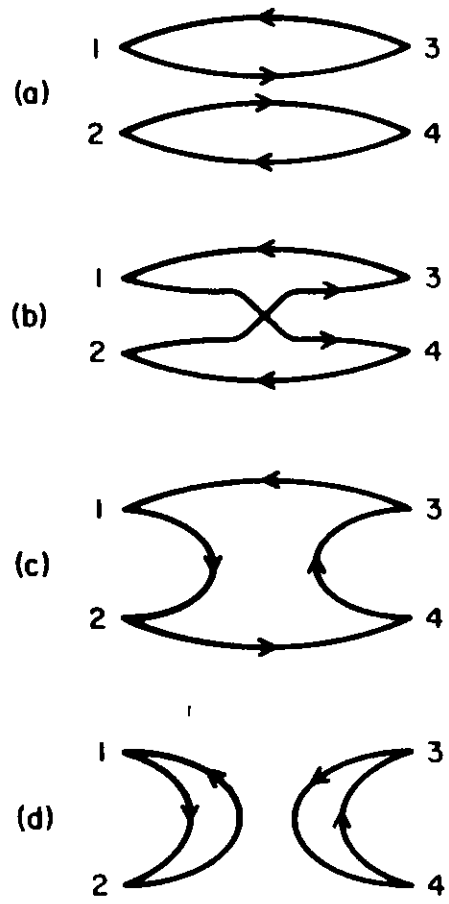

Figure 1. Diagrams contributing to two pion correlation functions: (a) "direct" or "gluon exchange"; (b) "crossed" or "quark exchange"; (c) "single annihilation": and (d) "double annihilation". The lines represent quark and anti-quark propagators in a background gluon field.

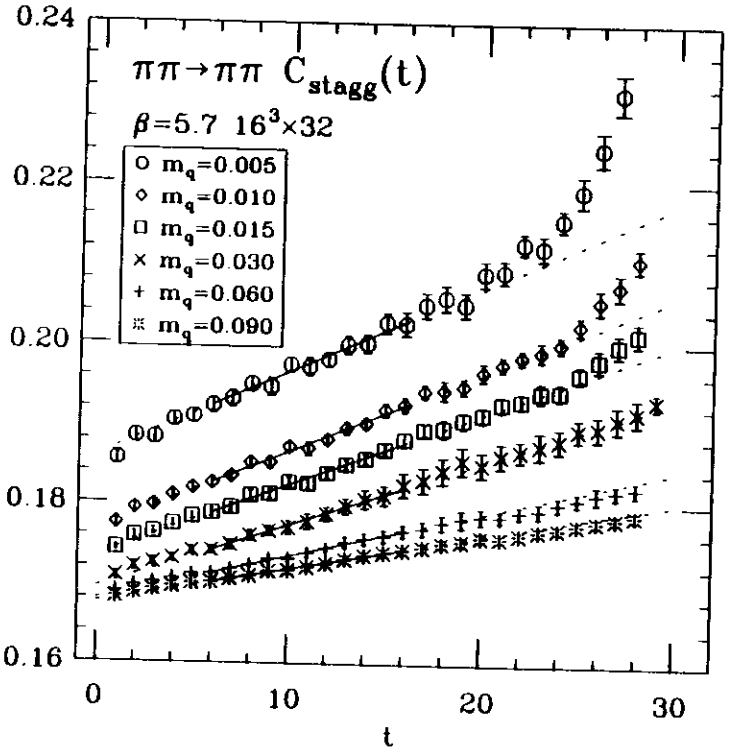

Figure 2a. The $\pi\pi \to \pi\pi$ crossed correlator $C_{stagg}(t) = C(t)/N_f$ on the $\beta = 5.7$, $16^3 \times 32$ lattices. The lines show the fits to the expected form, Eq. 6.13. The solid part of the line shows the region to which fitting was actually done, $t = 6 - 16$.

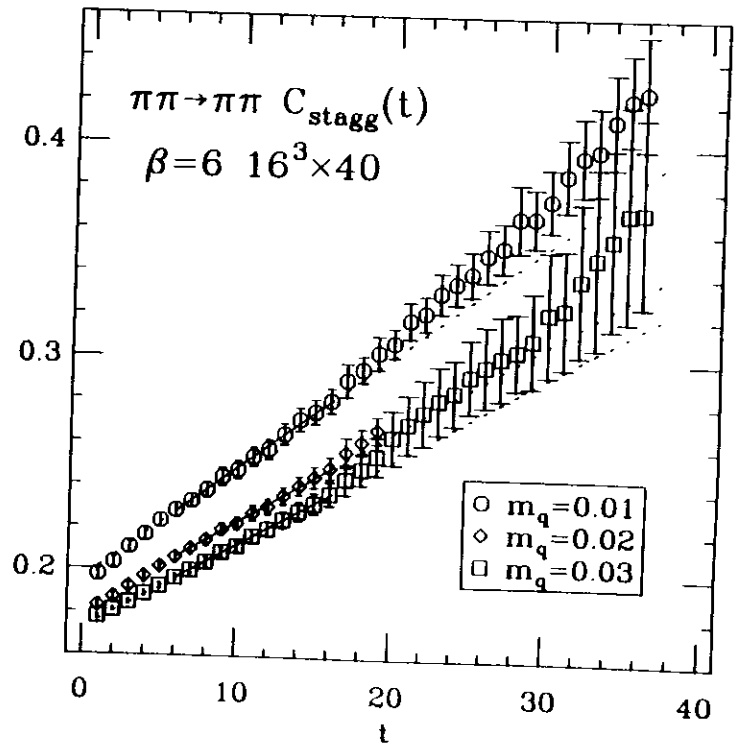

Figure 2b. The $\pi\pi \to \pi\pi$ crossed correlator $C_{stagg}(t)$ on the $\beta = 6$, $16^3 \times 40$ lattices (with some points at $m_q = 0.02$ removed for clarity). Notation as in Fig. 2a.

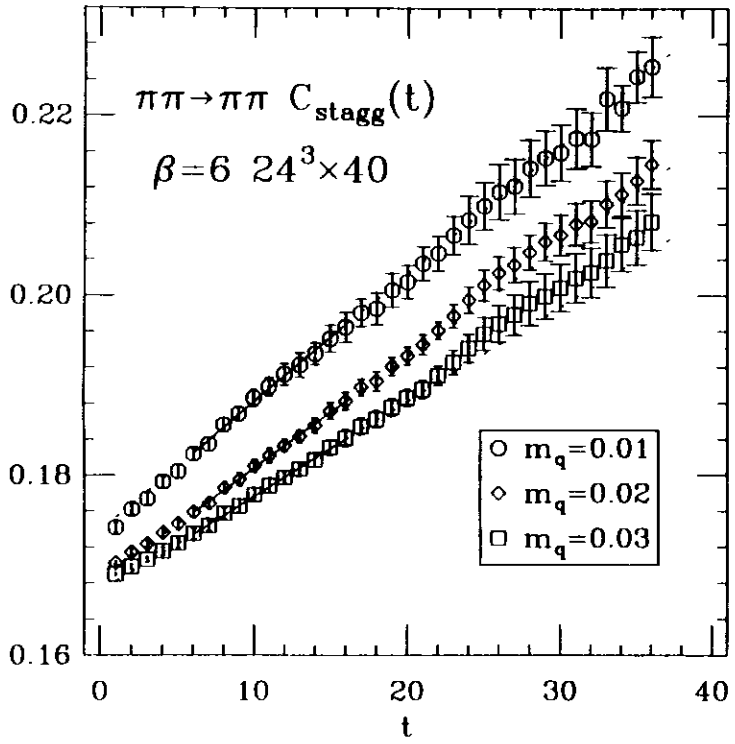

Figure 2c. The $\pi\pi \to \pi\pi$ crossed correlator $C_{\rm stagg}(t)$ on the $\beta = 6$, $24^3 \times 40$ lattices. Notation as in Fig. 2a

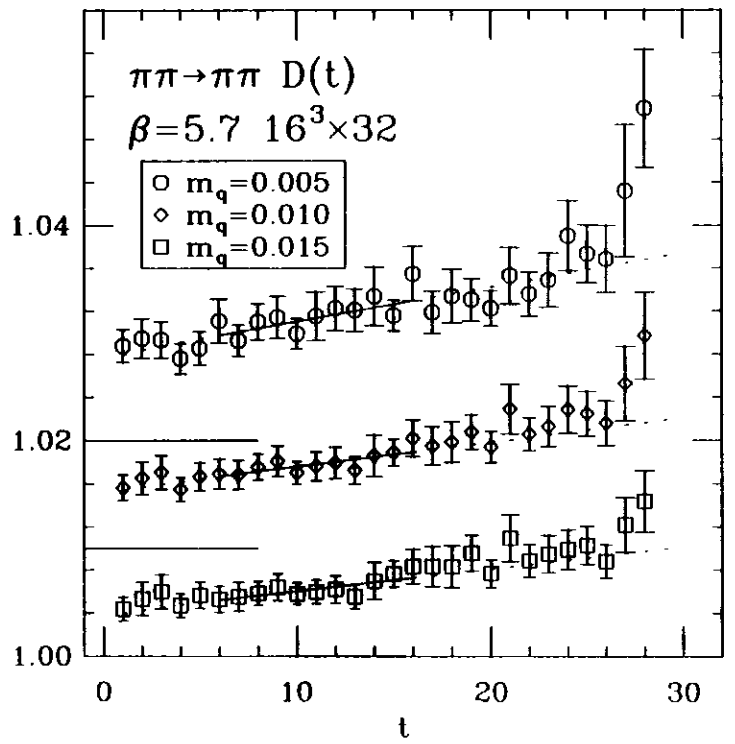

Figure 3a. Results for the $\pi\pi \to \pi\pi$ direct correlator $D(t)$ on the $\beta = 5.7$, $16^3 \times 32$ lattices. For clarity, points from the lightest two masses are vertically offset. The offset values of unity are indicated by the short horizontal lines. The lines show the fitted function (Eq. 6.13), including the curvature caused by $H(t)$, even though the fit is actually made to the linear approximation to this function in the fit range.

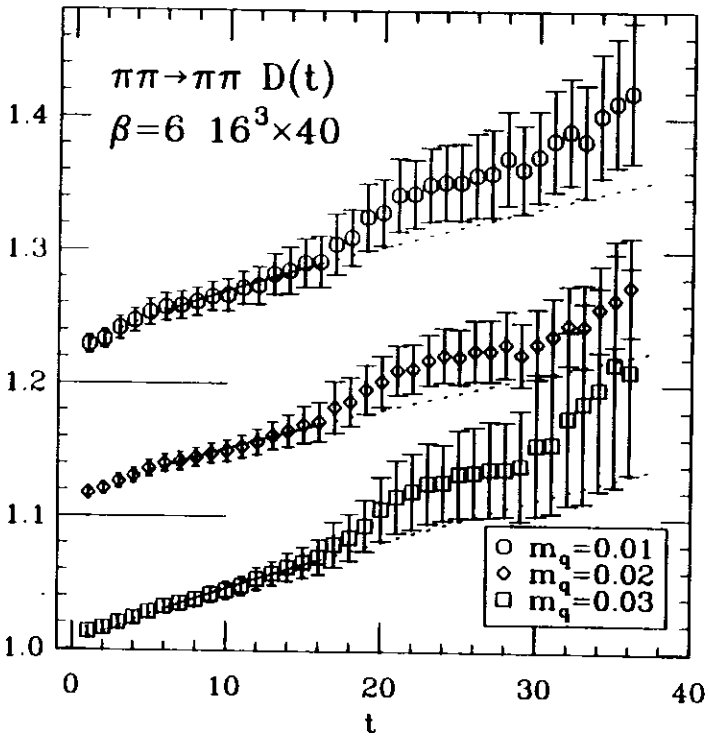

Figure 3b Results for the $\pi\pi \to \pi\pi$ direct correlator $D(t)$ on the $\beta = 6$, $16^3 \times 40$ lattices. Notation as in Fig. 3a.

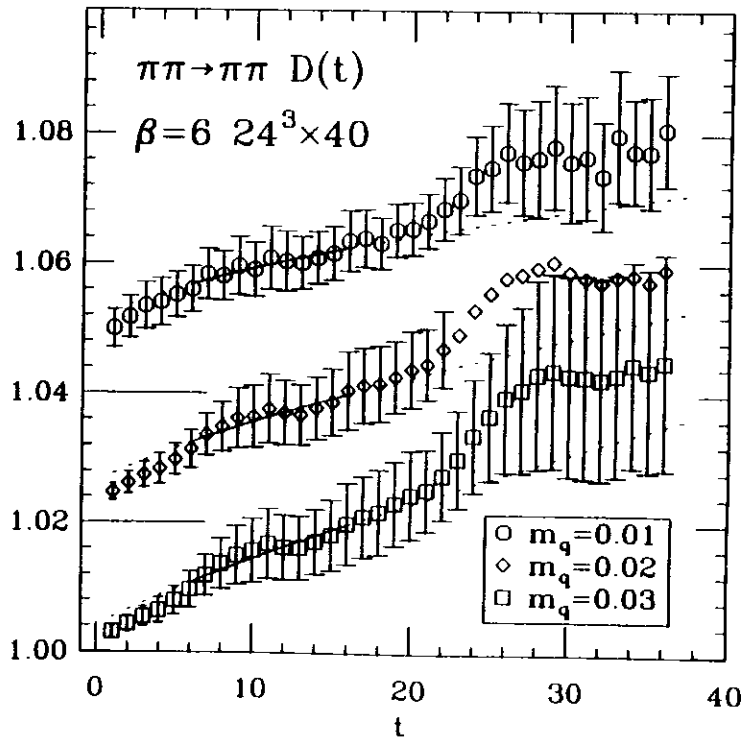

Figure 3c Results for the $\pi\pi \to \pi\pi$ direct correlator $D(t)$ on the $\beta = 6$, $24^3 \times 40$ lattices. Notation as in Fig. 3a. Some of the errors are excluded for clarity.

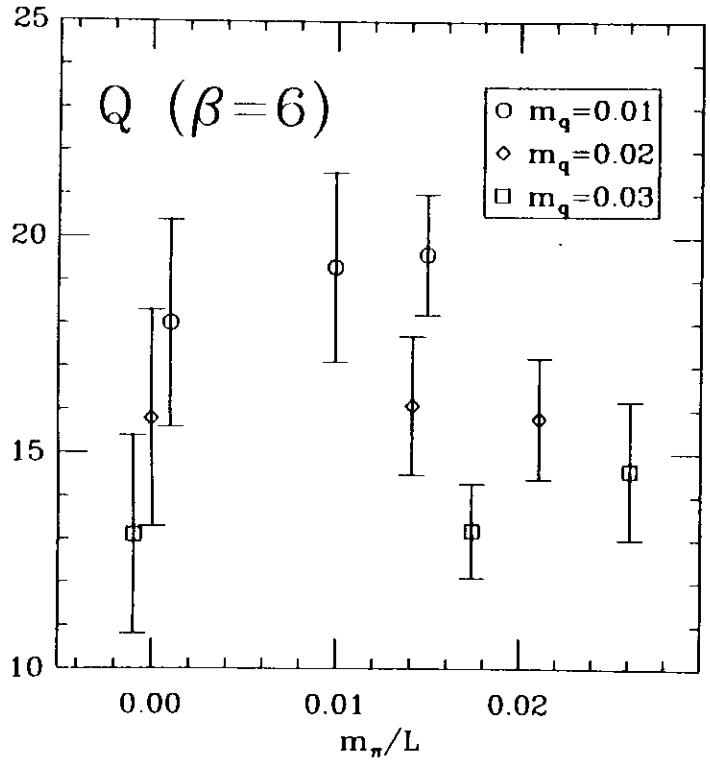

Figure 4. Volume dependence of Q at $\beta = 6$. The values at $m_\pi/L \approx 0$ (some offset horizontally for clarity) are the intercepts expected in the chiral limit: $Q(L = \infty) = 1/(16 f_\pi^2)$.

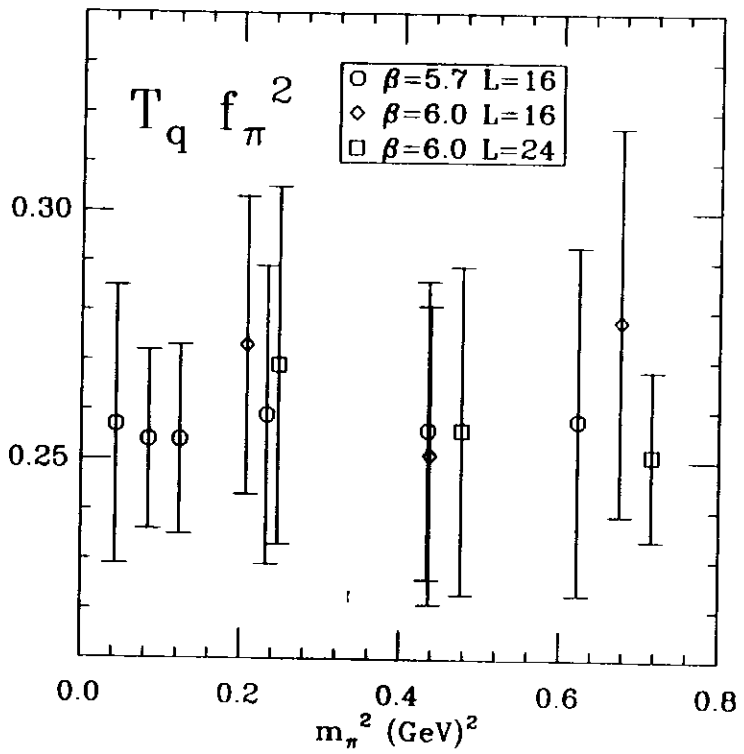

Figure 5. Testing the chiral prediction for the scattering amplitude. Results for $N_f Q f_\pi^2 = T_q f_\pi^2 + O(1/L)$. The expected chiral limit is 1/4.

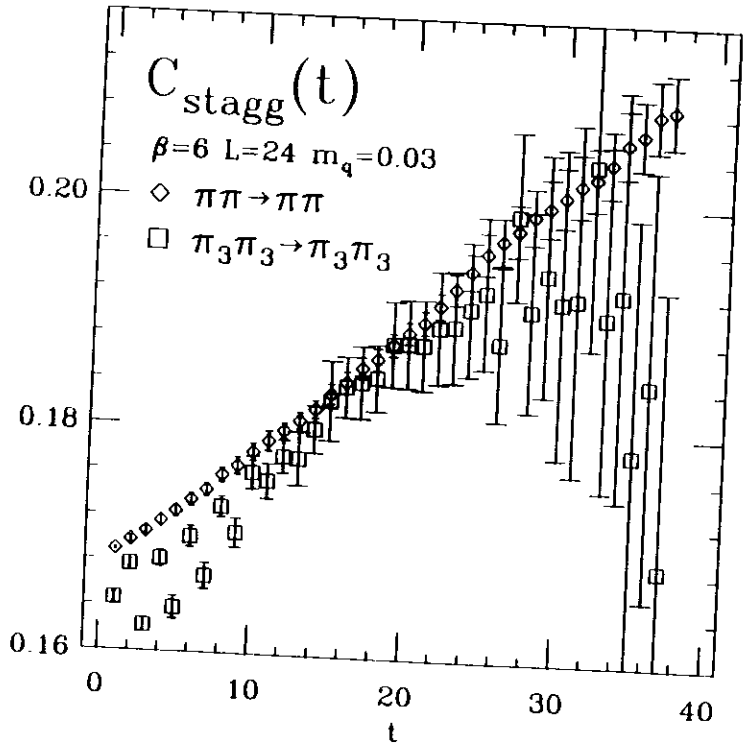

Figure 6a Comparing $C_{stagg}(t)$ for $\pi_3\pi_3 \to \pi_3\pi_3$ and $\pi\pi \to \pi\pi$ at $\beta = 6$, $L = 24$, $m_q = 0.03$. The solid line shows the expected result (not a fit) for the $\pi_3\pi_3 \to \pi_3\pi_3$ calculation using Eq. 6.13.

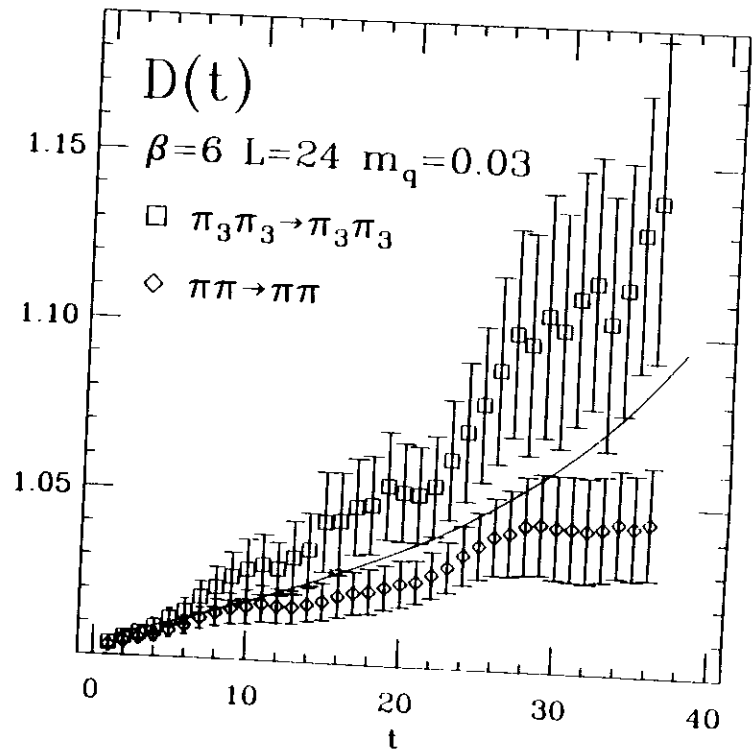

Figure 6b Comparing $D(t)$ for $\pi_3\pi_3 \to \pi_3\pi_3$ and $\pi\pi \to \pi\pi$ at $\beta = 6$, $L = 24$, $m_q = 0.03$. Notation as in Fig. 6a.

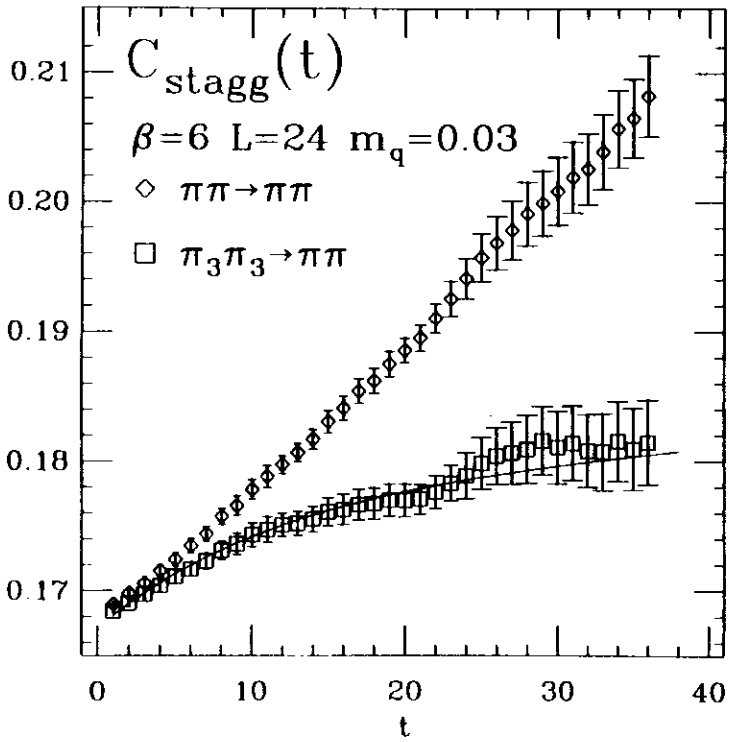

Figure 7a. Comparing $C_{stagg}(t)$ for $\pi_3\pi_3 \to \pi\pi$ and $\pi\pi \to \pi\pi$ at $\beta = 6$, $L = 24$, $m_q = 0.03$, together with the prediction from Eq. 6.13.

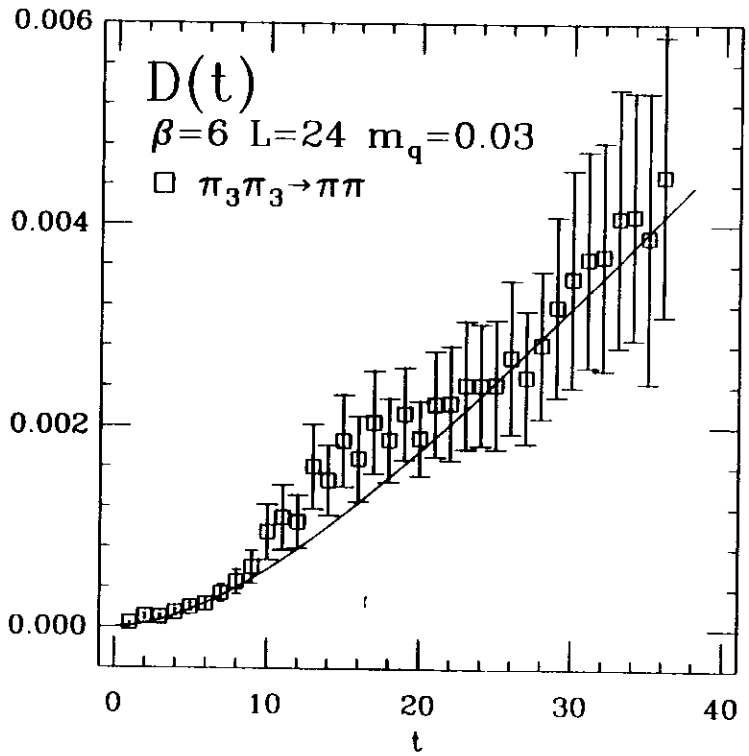

Figure 7b. Results for $D(t)$ for $\pi_3\pi_3 \to \pi\pi$ at $\beta = 6$, $L = 24$, $m_q = 0.03$, together with the prediction from Eq. 6.13.

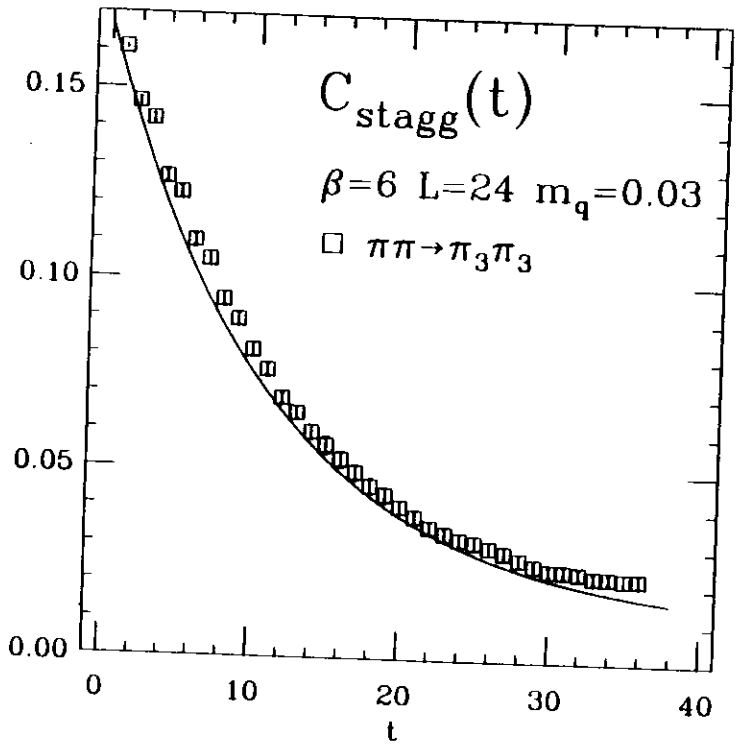

Figure 8a Results for $C_{stagg}(t)$ for $\pi\pi \to \pi_3\pi_3$ at $\beta = 6$, $L = 24$, $m_q = 0.03$, together with predictions from Eq. 6.13

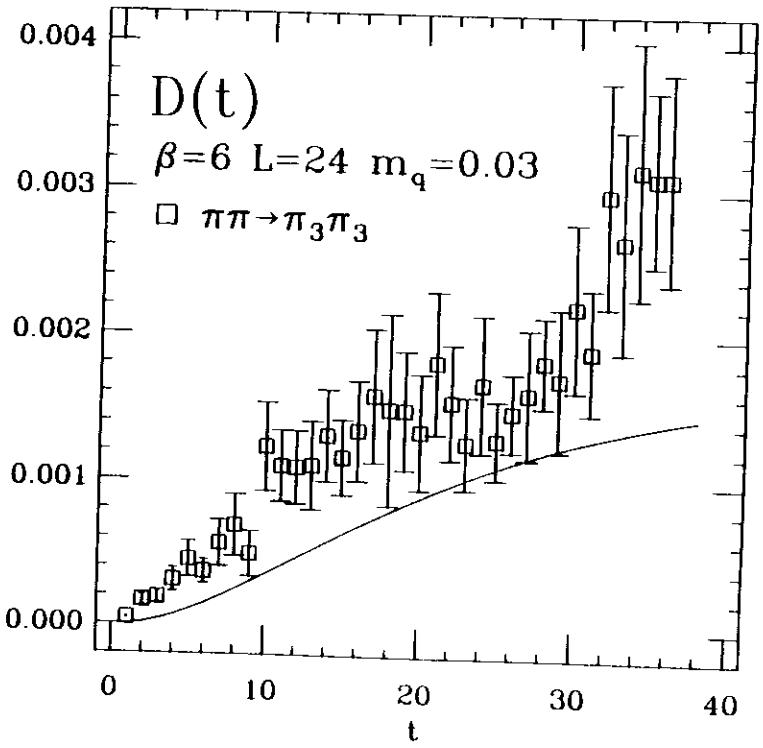

Figure 8b. Results for $D(t)$ for $\pi\pi \to \pi_3\pi_3$ at $\beta = 6$, $L = 24$, $m_q = 0.03$, together with predictions from Eq. 6.13